Cell calcium changes in response to endogenous and exogenous small molecules: Microfluidic single-cell monitoring and microplate bulk-cell measurement

by

Abolfazl Rahimi

B.Sc., Sharif University of Technology, 2019

Thesis Submitted in Partial Fulfillment of the
Requirements for the Degree of
Master of Science

in the
Department of Chemistry
Faculty of Science

SIMON FRASER UNIVERSITY
Fall 2023

Declaration of Committee

Name:	**Abolfazl Rahimi**
Degree:	**Master of Science**
Title:	**Cell calcium changes in response to endogenous and exogenous small molecules: Microfluidic single-cell monitoring and microplate bulk-cell measurement**
Committee:	**Chair: Robert Britton** Professor, Chemistry
	Paul C.H. Li Supervisor Professor, Chemistry
	Tim Storr Committee Member Professor, Chemistry
	Bingyun Sun Committee Member Associate Professor, Chemistry
	Neil R. Branda Examiner Professor, Chemistry

Abstract

Intracellular calcium ion ($[Ca^{2+}]_i$) is a messenger that regulates many cellular functions, and contributes to many biochemical cell processes. The measurement of calcium allows us to examine the responses of the cells to endogenous molecules (e.g. histamine) and exogenous molecules (e.g. cannabinoids). Measurement of $[Ca^{2+}]_i$ can be done on a microfluidic chip or a microplate reader by monitoring the emitted fluorescence from the calcium-Fluo4 chelate formed inside the cell. While the calcium measurement is conducted on a single cell captured within a microchip chip, the microplate experiment is performed in a 96-well plate and each well contains around 40,000 cells and provides an average value for the cell response. The high number of cells in a microplate will allow researchers to perform bulk calcium analysis. On the other hand, the single-cell method by a microfluidic glass chip has advantages such as small reagent consumption and fast analysis. The combination of microfluidic single-cell and bulk-cell analysis of calcium will reveal detailed information about calcium concentration in two different scales. This allows us to examine the difference in cell responses obtained from two types of lung cancer cells, namely A549 cells and ACE2-enriched A549 cells.

Keywords: Intracellular calcium measurement; Single-cell; Bulk-cell; Lung cancer cells; Microfluidic chip; microplate reader

Dedication

تقدیم به پدر و مادر عزیز و مهربانم که در سختی ها و دشواری های زندگی همواری یاوری دلسوز و فداکار و پشتیبانی محکم و مطمئن برایم بودند.

و با احترام و تواضع تقدیم به همه آزادگانی که مرگ با عزت را به زندگی با ذلت ترجیح دادند.

و تقدیم به عزیزی که روزی گفت: یک برادر کرمانی ما داریم خیلی رک حرف میزنه. همینطور یقه ات رو میگیره تکون هم میده حرف میزنه. گفت فلانی! همه رو فرستادی. خودت موندی. من خیلی...آتش گرفتم. گفتم چیکار کنم؟ حیفه حقیقتا بمونیم حیفه.

Acknowledgements

I would like to express my heartfelt gratitude to my beloved father and mother whose unwavering support has been a cornerstone of my life's journey. Their encouragement, love, and belief in me have been a constant source of strength, and I cherish the bonds we share. I am also thankful to my loyal friends for their support and kindness in all these years.

I am also immensely grateful to my beloved country, IRAN, and its remarkable people. Iran has given me the invaluable gift of access to free and high-quality education. This opportunity has shaped my perspective, broadened my horizons, and empowered me to pursue my dreams. The rich cultural heritage, warm hospitality, and resilient spirit of the Iranian people have always filled my heart with pride and a sense of belonging.

Furthermore, I am grateful to the members of my supervisory committee, Dr. Tim Storr and Dr. Bingyun Sun and my senior supervisor Dr. Paul C.H. Li and Dr. Neil R. Branda as internal examiner and Dr. Robert Britton as defence chair, whose guidance and mentorship played a pivotal role in my successful completion of my master's program.

Table of Contents

List of Tables

List of Figures

List of Acronyms

ACE2	Angiotensin converting enzyme 2
AM	Acetoxymethyl
Ang(1-7)	Angiotensin (1-7)
AT1	Angiotensin 1
AT2	Angiotensin 2
BCE	Beta-caryophyllene
CBC	Cannabichromene
CBD	Cannabidiol
CBG	Cannabigerol
CBL	Cannabicyclol
CBN	Cannabinol
CCD	Charge-coupled device
CE	Capillary electrophoresis
DMSO	Dimethyl sulfoxide
ED	electrochemical detection
EOF	Electroosmotic flow
FBS	Fetal bovine serum
FC	Flow cytometry
GPCR	G-protein coupled receptor
HBSS	Hank’s balanced salt solution
HPLC	High Performance Liquid Chromatography
IP3	Inositol 1,4,5-trisphoshate
LME	Limonene

LOC	Lab-on-a-chip
MYR	Myrcene
NCX	Na^{+}/Ca^{2+} exchanger
PIP2	Phosphatidylinositol 4,5-bisphosphate
PLC	Phospholipase C
PMCA	Plasma membrane Ca^{2+} ATPase
PMT	Photomultiplier tube
PTP	Permeability transition pore
RAS	Renin-angiotensin system
RYR	Ryanodine receptors
SARS-CoV-2	Severe acute respiratory syndrome coronavirus 2
SERCA	Sarcoplasmic/ endoplasmic reticulum Ca^{2+} -ATPase
Si	Silicon
SOC	Store-operated Ca^{2+} channels
SR	Sarcoplasmic reticulum
TCD	Thermal conductivity detector
THC	Tetrahydrocannabinol
μTAS	Micro total analysis system

Chapter 1. Introduction

Intracellular calcium ion ($[Ca^{2+}]_i$) serves as an important messenger governing a multitude of cellular functions and influencing numerous biochemical processes. To measure $[Ca^{2+}]_i$, different methods are employed, such as microfluidic chips and microplate readers, which monitor the emitted fluorescence resulting from the formation of the calcium-Fluo4 chelate within the cell. The quantification of calcium levels enables us to explore cellular responses to both endogenous and exogenous stimuli. The integration of microfluidic single-cell and bulk-cell analyses for calcium measurement provides a comprehensive view of calcium concentration at two different scales which will be elaborated in this thesis.

1.1. Single-cell Analysis

Scientists mainly obtain information about cell behaviours in bulk assays using thousands or millions of cells. For instance, by usage of the cytotoxicity assay using 3-[4,5-dimethylthiazol-2-yl]-2,5-diphenyl tetrazolium bromide (MTT), scientists typically average the results of large groups of cells to obtain information about the behaviour, status, and health of individual cells. Bulk methods are used because they are straightforward and convenient ways of determining how cells behave. [1]

However, the nature of cells is heterogeneous. Cells in populations differ in function and destiny. Examples of cell heterogeneity include responses to a specific stimulus (such as medication) or gene expression among different cells. Due to this cell heterogeneity, conventional biochemical experiments that examine cell populations sometimes miss the variability and heterogeneity of cells.[1]

One approach to overcome the aforementioned problems is to reduce the scale of assays for single cell analysis which can be achieved by microfluidics or “lab-on-a-chip” technology. Microfluidics has been used to perform a variety of biological assays with minimal reagent consumption. In particular, the dimensions (10−100 μm) of microfluidics have made assays of biological cells a popular application. Unfortunately, cell assays, like other microfluidic methodologies, have suffered from limited means to manipulate fluids and cells. [2]

While intracellular signaling mechanisms and transcriptional modifications can take minutes or hours, early events in cell signaling (i.e. calcium signaling) can happen seconds after the stimulation. Understanding the highly dynamic mechanisms that regulate cell variability and fate requires multi-parameter experimental and computational methods that include quantitative measurement with stimulation of cells by various biochemical stimuli.[3]

1.1.1. Fluorescence detection for single-cell analysis

Since cells are very small (diameter, 7-200 μm; volume, fL~nL), the analysis and detection of intracellular components of single cells demand high-sensitivity detectors. For instance, laser-induced fluorescence (LIF), [4, 5, 6] fluorescence, and electrochemical detections are the most broadly used detection methods in single-cell analysis. In the next chapters of this thesis, the use of fluorescence detection and the instrumentation setup to study the dynamics of intracellular components of single cells will be elaborated. [7, 8]

Most intracellular species (e.g., Ca^{2+} or amino acids) do not have intrinsic fluorescence. To measure non-fluorescent molecules by fluorescence, a fluorescent probe is needed to label them. For example, several fluorescent Ca^{2+} dyes have been developed, namely, Fluo 4, Fluo-3, Calcium green, Quin 2, Indo 1, Fura 2, and Calcium 3, to measure the cytosolic Ca^{2+} concentration and act as a fluorescence probe.[9] Among all the previously mentioned probes, Fluo-4 is one of the most common Ca^{2+} indicators with green emission at 530 nm when excited at 470 nm. Fluo 4 is negatively charged and is cell impermeable. Fluo 4 forms a permeable molecule of Fluo 4 AM ester that can pass through the cell membrane by modification with the acetoxymethyl (AM) ester group.[10] The chemical structure of Fluo 4 AM is shown in Figure 1.1. Once Fluo 4 AM ester is loaded inside the cells, four acetoxymethyl groups will be hydrolyzed to produce Fluo-4, which forms a fluorescent complex with binding by the cytosolic Ca^{2+} ion. Previous studies have also demonstrated that Fluo 4 specifically binds with intracellular calcium ion in presence of other intracellular cations.[11] In later chapters, this method will be used to

measure $[Ca^{2+}]_i$, in single cells microfluidic chip by fluorescence.[12]

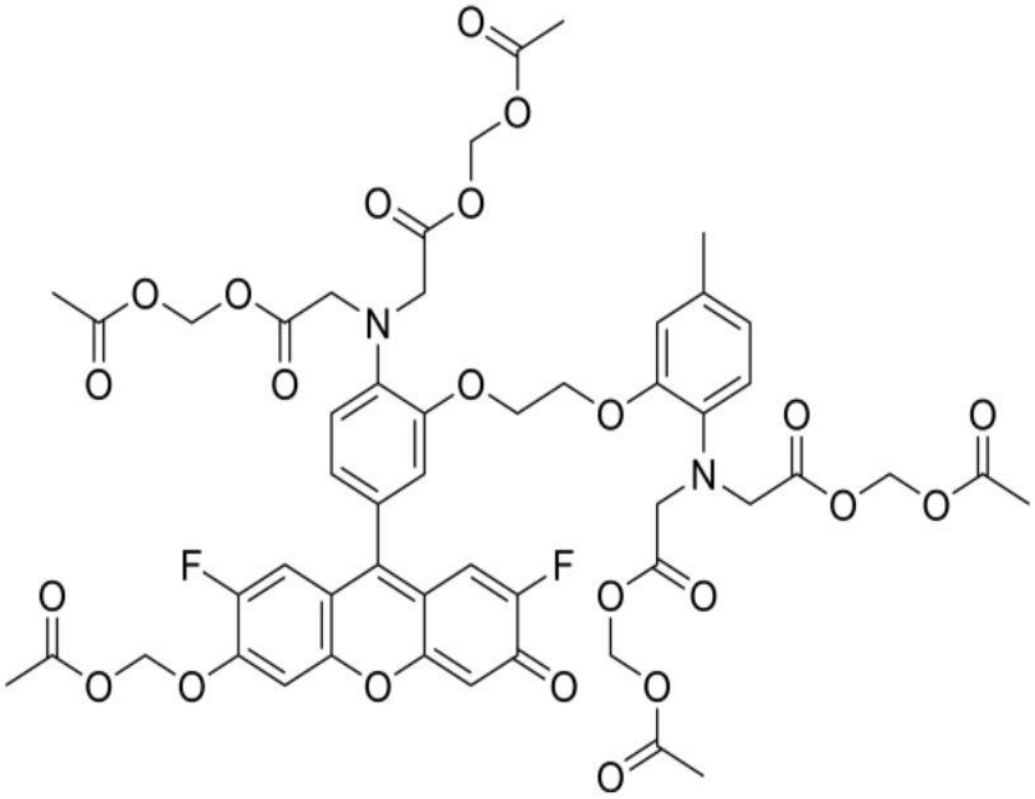

Figure 1.1. Chemical structure of Fluo 4 AM ester

Fluo 4 AM ester itself does not bind Ca2+, but it is readily hydrolyzed to Fluo 4 by endogenous esterases once inside cells according to Figure 1.2 . Fluo 4 is essentially nonfluorescent without Ca2+ present, but the fluorescence elevates Ca^{2+} binding.[9] Fluo 4 has a high rate of cell permeability and high fluorescence emission. The dissociation constant of Fluo 4 is 0.35μM which shows that the binding affinity of Fluo 4 with calcium is relatively strong.[13] Because of its high fluorescence emission intensity, Fluo 4 can be utilized at lower intracellular concentrations which makes it a minimally invasive calcium indicator.[14]

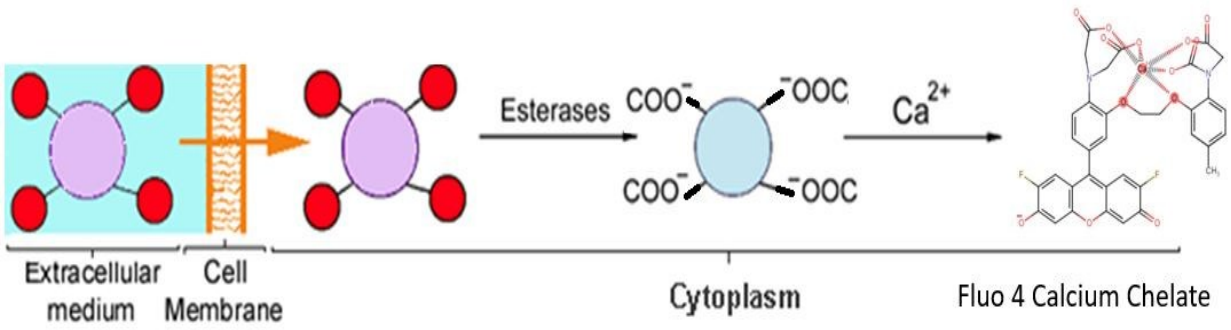

Figure 1.2. Fluo 4 dye loading process

1.1.2 Techniques for Single-cell Analysis

The most popular methods for single-cell analysis are flow cytometry (FC), and slide-based microscopy.[15] Flow cytometry is a high throughput method for single-cell research that offers insightful quantitative data on cell distribution. On the other hand, flow cytometry typically provides researchers with a single point of information at a time about a population of cells but is unable to provide the same cell's time-dependent information. Furthermore, flow cytometry can't be used for manipulating a single cell. These drawbacks restrict its use in dynamic single-cell analysis. [16]

Slide-based microscopy can offer a numerical understanding of cellular behaviours. Slide-based microscopy can also provide time-dependent dynamic information on individual living cells. In addition, microscopy can reveal details about cell morphology. As a result, microscopy techniques can monitor the responses of cells to drug-candidate compounds in a high-content screening manner.[17] But microscopy cannot offer the same throughput as flow cytometry and also it is challenging to analyze suspension cells on microscopic slides.[18]

As for single-cell analysis, there are more methods, including microfluidic lab-on-a-chip and capillary electrophoresis. [18] Samples either lysed for sampling or directly sampled before chemical separation and CE detection of the analytes in a capillary. However, capillary electrophoresis (CE) is unable to measure the dynamic responses of live cells in real-time. On

the contrary, the recently developed method of microfluidic lab-on-a-chip is more than a chemical separation method. It also provides a single-cell platform for dynamic analysis. [6, 19, 20]

1.2. Microfluidic Lab-on-a-chip

Recent miniaturization technology has been able to reduce reagent costs, to provide integration and automation, to enhance analytical speed and performance, and to enhance throughput.[21, 22]

In 1979, the first miniaturized GC column with a silicon (Si)-based thermal conductivity detector (TCD) was built and tested. [23]A microscale HPLC column with a conductometric detector was built on a silicon wafer in another related work. Hence, the "micro total analysis system" (μTAS),[24] which combines sample pre-treatment, separation, and detection, was proposed by Manz et al. Later, such a system was referred to as a "microfluidic chip" or "Lab-on-a-chip (LOC)". The first liquid-based LOC system demonstration was based on CE separation of calcein and fluorescein was accomplished on a glass chip with a 10-μm deep and 30-μm broad channel and detected by LIF in 6 min. [25, 26] The success of the aforementioned LOC was attributed to electroosmotic flow (EOF), which is used to pump reagents in the micron-scale capillaries.

Since then, numerous current detection techniques, including, fluorescence, LIF, and electrochemical detection (ED), have been coupled to microfluidic chips. Additionally, various CE modes have been demonstrated in miniature devices. Other than chemical separations, various research groups have succeeded in cellular, genetic, and protein analysis, immunoassay, and clinical diagnosis, as summarised in numerous review papers and books. [27, 28, 29] Additionally, rather than being created for biochemical analysis, the microchips were created as micro reactor chips for chemical synthesis. [30]

1.2.1. Advantages of microfluidic chips

The term "biochips" generally encompasses LOC and microarray devices. Accordingly, the microfluidic chip is also called the microfluidic biochip, which has several advantages as follows: [31 32]

1. Low reagent consumption (μL) with low cost.

2. Low sample usage (down to 100 cells) for bioanalysis, especially when the biological samples are limited.

3. Better choice in performing different biological routine operations. For instance, the Fluo-4 dye loading process can be done with minimal cell damage in microfluidic chip.

4. Integration of several techniques (e.g., cell retention, detection, mixing, and pumping) on one microchip.[47]

5. Fast and real-time analysis. For instance, Harrison et al. separated six amino acids within 15 seconds by a microchip-based CE system. [2]

6. Parallel and high throughput process by utilizing multiple channels, which will reduce the time for analysis and the experiment cost.[19, 32]

7. High performance and high efficiency in chemical separation applications.

8. Miniaturization and portability of the devices for in-situ analysis and diagnosis.

9. Automation and flexible design by modern MEMS (Micro-Electro-Mechanical Systems) technology.

These advantages depend on the application and may not be applicable in all cases.

1.3. Microfluidic single cell analysis

The major part of research papers on microfluidic devices has been focused on the pharmaceutical, life, biological, and clinical sciences. [27] During the 1990s vast majority of research work was focused on amino acids, [21] genetic analysis,[33 34] and then protein analysis.[35] In the past few years, the analysis of even more complex biological systems, such as live cells, using microfluidic biochips has attracted great interest among scientists. As an example patch clamping is used to study ion channels and this technique involves careful positioning of a fine-tipped glass micropipette onto the surface of the cell and the throughput can be increased by utilizing microfluidic and on-chip single cell analysis.[36, 37]The application of microfluidic technology has already entered the life science field and has become a driving force for cellular biology, neurobiology and pharmacology discoveries. Because of the small dimensions of the microfluidic channels (10-100 μm), they are compatible with the cell sizes, and the cell-based

microfluidic assay has become a popular μTAS application since 2002. [27] Different applications of microfluidic assays are listed in Table 1.1.

Table 1.1 The application of microfluidic biochips in cell-based assays

Application	Limitations	References
Cell culture	small molecules diffusing into the PDMS	[38]
Cell trap and retention	imperfect retention	[8, 39]
Cell transport	Cell adhesion to the chip	[40]
Malaria-Infected erythrocytes	microscopes are hard to transport to very remote areas	[41]
Patch-clamp recording	Low current resolution	[36,37]
Cell electroporation	Negative effect on cell viability	[42, 43]
Cell fusion	reduced fusion efficiencies	[44]
On-Chip PCR	High cost and low accessibility	[45]
Electrical stimulation of muscle cells	difficult to dose properly	[46]
Cell sorting	Slow response speed	[47]

Cell lysis	Time consuming	[48]

Due to cell heterogeneity much focus of microfluidics-based cellular applications has been put on single-cell analysis as summarized by several review articles. [49] [50]

1.3.1. Cell Transport

Currently, two main approaches exist for cell transport in microfluidic channels to specific locations. The first approach is the electrokinetic method.[51] The aforementioned method has some disadvantages, such as gas bubble formation in the solution. The second approach for cell transport is the hydrodynamic method. This is a much gentler method to the cells which causes minimal cell damage, so I have utilized this method to transport cells in this research work. [52]

1.3.2. Cell Retention

Cell retention can be achieved by the hydrodynamic methods using physical structures (such as slit, weir and V-shaped structure). Figure 1.3 shows a single A549 cell retained in a V-shaped structure on a microfluidic chip.

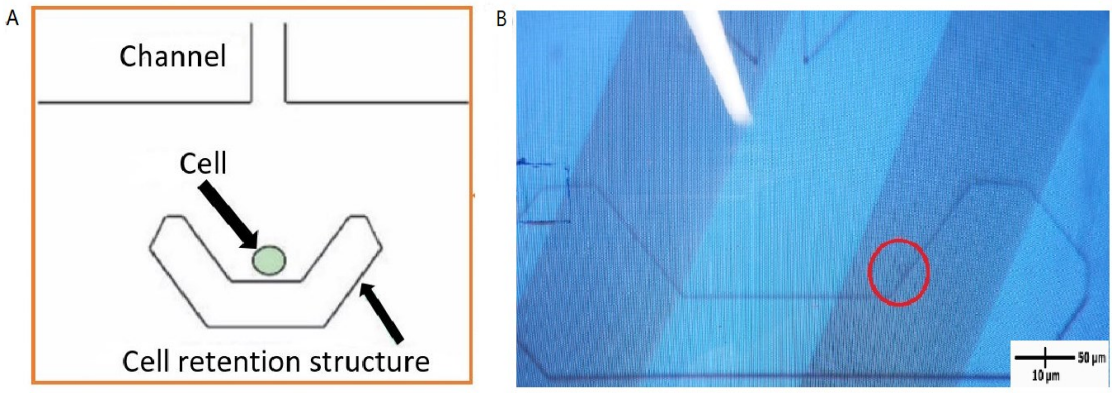

Figure 1.3. A) Schematic diagram of V-shaped cell retention structure B) V-Shaped cell retention structure under microscope

In addition, cell adhesion, optical trapping" and dielectrophoresis (DEP) have been exploited to retain cells. Among them, hydrodynamic cell retention by physical structures is commonly used, as summarized in Table 1.2.

Table1.2. Table of different hydrodynamic cell retention methods

Retention method	Particles of interest	Applications	Limitations	References
Weir	U937cell, Jukart T cell	Intracellular Ca^{2+}	Passive retention. Undesired cells may be trapped.	[1]
Weir	Muscle cell	Dynamic cytosolic Ca^{2+} mobilization	Not suitable for small sized cell retention	[7]
Slit	WBC, RBC	PCR	Passive retention. Unable to obtain individual cell retention. Cells were deformed and passed through.	[53]
Dam	HL-60 cell	ATP-stimulated Ca^{2+} uptake	Passive retention. Inability to obtain individual cell retention. Closely docked cells can interfere with the measurement of their adjacent cells.	[54]
V-shaped structure	Muscle cell, RAW cell	Dynamic cytosolic Ca^{2+} mobilization	Cell retention was not strong enough for complicated multistep analysis of muscle cells.	[7,]

In one paper regarding a glass-Si chip, white blood cells (WBC) and latex beads (6 μm in diameter) were retained at the 5-μm spacing slits within a 500-μm channel. But the cells tend to deform and pass through the slits in the study of red blood cells (RBC). Hence, these slit-type structures are hard to retain and isolate single cells, consequently these structures are seldom used in single-cell analysis. [55]

Yang et al. also designed a dam structure in a quartz microchip for cell retention. Despite usual perpendicular dam structure or weir, the cells docked along a parallel dam were under less shear stress according to Figure 1.4. In this work, Ca^{2+} uptake in HL-60 cells, as stimulated by ATP (adenosine triphosphate) was studied. Unfortunately, this parallel dam structure can't immobilize a single cell, and very closely-docked cells can interfere with the fluorescence measurement of their adjacent cells.[53]

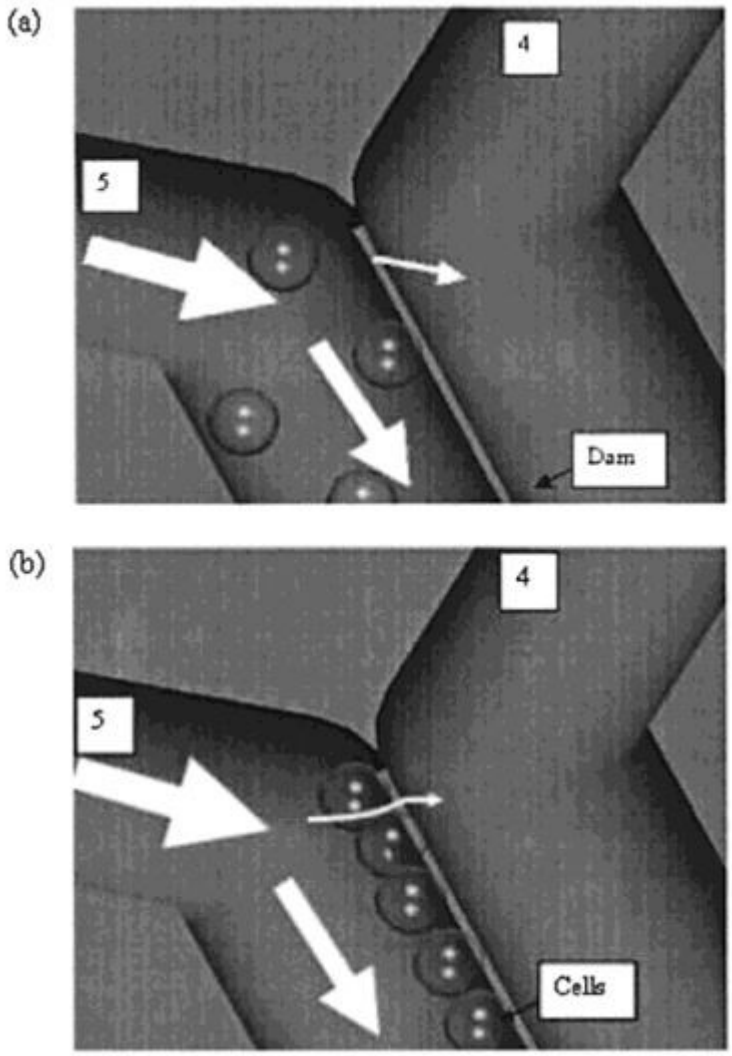

Figure 1.4. Schematic diagram of the fluid flow during cell docking. (A) The hydrodynamic pressure difference can bring the cells in channel 5 to dock alongside the dam. (B) The fraction of flow across the dam is reduced and excessive cells are driven along the main flow rout.[53] Reprinted with permission from the American Chemical Society.

In 2003, Wheeler et al. fabricated and designed a U-shaped trapping structure in PDMS to isolate and retain a single cell according to Figure 1.5. The main channel and the cell dock are 20 μm deep, while the drain channel (or weir) is 5 μm clearance. A single mammalian cell (Jurkat T cell, 15 μm in diameter) has been immobilized and trapped in the U-shaped structure. Utilizing this cell retention method, the ionomycin (IM)-mediated [Ca^{2+}] flux in different cells was analyzed and measured. [1]

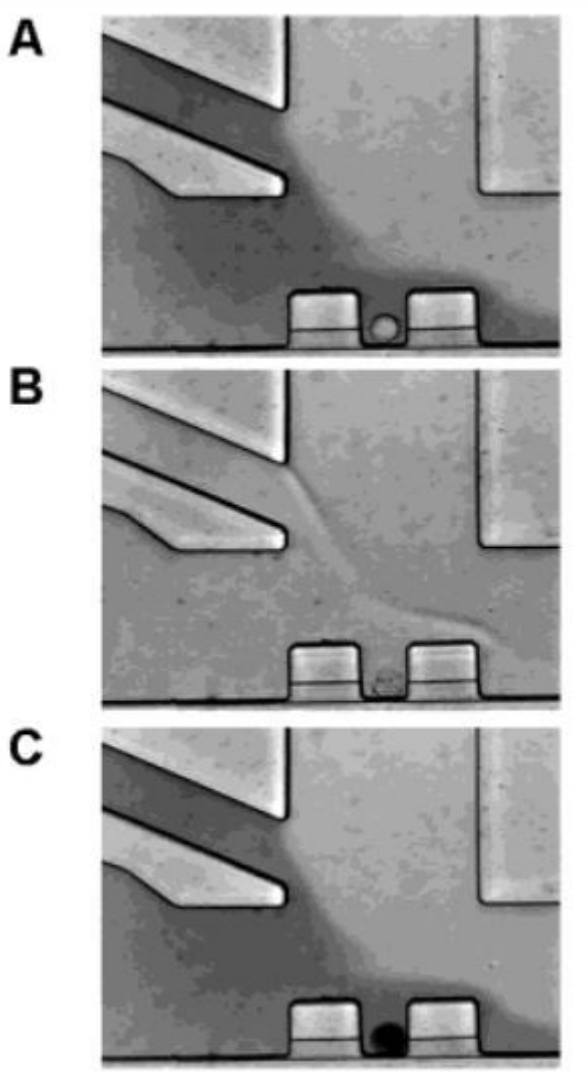

Figure 1.5. Viability assay on a single Jurkat T-cell. (A) Live cell perfused with trypan blue. (B) Methanol added which causes cell death. (C) Dead cell stained with trypan blue.[2] Reprinted with permission from the American Chemical Society.

All the aforementioned hydrodynamic trapping methods utilizing slits and weirs are passive trapping methods. These trapping microstructures are not useful to select and retain a desired single cell. Therefore, in this research an active hydrodynamic trapping approach is used which will be discussed in detail in later chapters.

1.4. Introduction to Bulk Cell Calcium Assays:

Bulk cell calcium assays enable researchers to perform measurement of calcium dynamics in populations of cells simultaneously. These assays provide a high-throughput approach to studying calcium signaling and can offer several advantages over single-cell measurements. Bulk assays provide a broader understanding of the calcium response within a cellular population, encompassing and averaging the overall cellular behaviour and heterogeneity present in the system instead of focusing on individual cells.[56]

1.4.1. Advantages of Bulk Cell Calcium Assays:

High-Throughput Capability: One of the important advantages of bulk cell calcium assays is their ability to handle large numbers of samples simultaneously. Microplate readers equipped with fluorescence, luminescence, or absorbance detection enable fast measurements of multiple samples in a high-throughput manner.[56] Fluorescence happens when an excited molecule, atom, or nanostructure, relaxes to the ground state through emission of a photon while electron spin remains same. On the other hand, luminescence is the spontaneous emission of radiation from an electronically excited species which is not in thermal equilibrium with its environment.[5] In drug discovery the previously mentioned capability is particularly beneficial because it can screen large compound libraries and can evaluate diverse experimental conditions.[57]

Time-Efficiency and Cost-Effective: Bulk assays reduce experimental time and cost significantly compared to single-cell measurements. By simultaneous measurement and analysis of the calcium response in multiple wells of a microplate researchers can gather data from numerous samples in a single experiment. This efficiency enables researchers to minimize experimental variability for fast and precise measurements.[58]

Population Behavior: Individual cells within a population may exhibit variations in their calcium responses due to environmental, genetic or other factors. Bulk assays reveal the overall trends and average responses, emphasizing the collective behavior and importance of calcium signaling in the system, by studying calcium dynamics at the population level.[59]

Sensitivity and Dynamic Range: Microplate readers used in bulk assays provide high sensitivity and a wide dynamic range of detection, which allow the measurement of subtle changes in calcium concentration. Fluorescent indicators and luminescent probes used in these assays provide excellent signal-to-noise ratios, enabling the detection of both transient and sustained calcium responses. This sensitivity in capturing subtle cellular responses and accurately characterizing the dynamics of calcium signaling is significantly improved.[60]

Flexibility and Versatility: Bulk cell calcium assays are versatile and are capable of being adapted to various experimental designs and cell types. Scientists have the option to choose from a wide range of calcium indicators including synthetic dyes and genetically encoded probes based on the specific needs of their study. Hence, microplate readers can be equipped with different detection modes which allow the measurement of luminescence, fluorescence, or absorbance signals.[61] Figure 1.6 illustrates the differences between single cell and bulk cell calcium measurement.

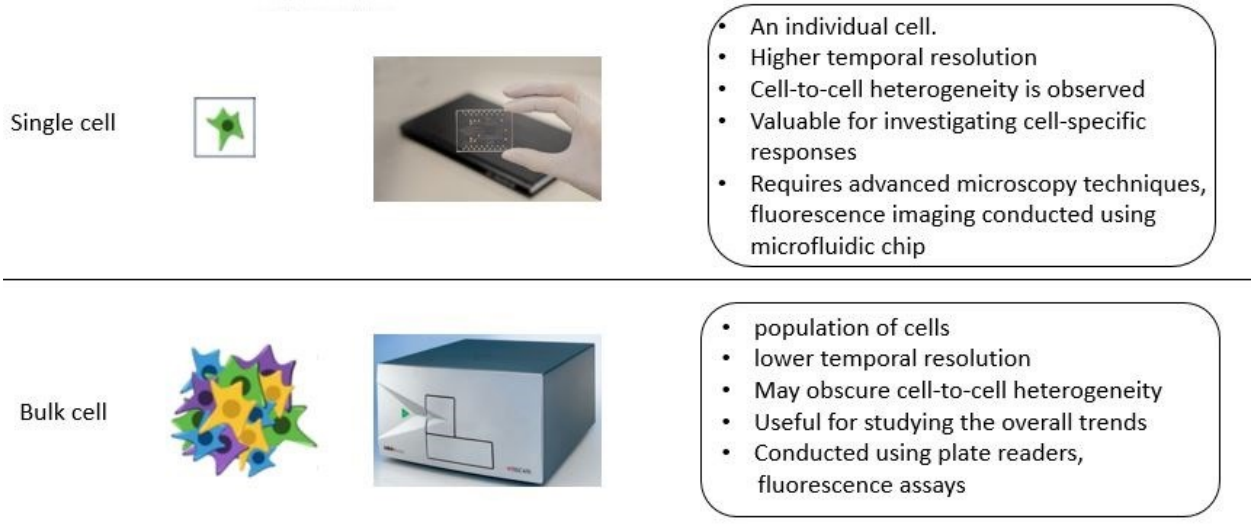

Figure 1.6. Differences between single cell and bulk cell calcium measurement

1.4.2. Experimental procedure of bulk cytosolic calcium concentration:

Experimental Design:

The assay begins with the selection of appropriate cell types and defining the experimental conditions. Design factors including cell culture conditions, treatment protocols, and desired temporal resolution should be considered at this stage.[62, 63 ,64]

Cell Preparation and Seeding:

The cell lines of interest for the experiment are cultured and prepared for the assay. These cell lines might be derived from primary cells, transfected cells, or stem cells, depending on the specific research question. Proper cell maintenance and culture techniques are crucial to ensure cell health, viability and functionality during the experiment. Cells will be seeded on a black multiwell plate with clear bottom, which is suitable for fluorescence measurement.

Calcium Indicator Loading:

Calcium indicators are very important for detecting changes in intracellular calcium concentration. Cell loading with a calcium indicator is a critical step in the assay. Commonly used calcium indicators include synthetic dyes (e.g., Fluo 4, Fura 2). These dyes can bind to the intracellular calcium and give rise to fluorescent emission. The choice of calcium indicator depends on several factors including the desired fluorescence properties, cell type, and experimental conditions.

Stimulation and Treatment:

The cells are often subjected to specific stimulation or treatment protocols to elicit calcium responses. This can involve the treatment with neurotransmitters, hormones, agonists, antagonists, or environmental cues that are the main concern of the research question. The timing, concentration, and duration of the stimulation are carefully controlled to achieve meaningful results.

Imaging Setup:

The bulk cell intracellular calcium assay typically involves fluorescence microscopy or a microplate reader system for obtaining data. Cells are loaded onto a suitable imaging platform, such as a glass-bottom dish or a multi-well plate. The imaging setup includes appropriate filters and excitation sources to selectively visualize the emitted fluorescence of the calcium indicator.

Data Acquisition and analysis:

The imaging system captures the fluorescence emitted by the calcium indicator in regards to changes in intracellular calcium concentration. The imaging parameters, such as exposure time, gain, are optimized to achieve the desired temporal and spatial resolution. The acquired images or fluorescence intensity measurements provide the raw data for subsequent calculations.

Interpretation and Conclusion:

The final step involves interpretation of the results obtained from the bulk cell calcium analysis. The data can provide information on cellular responses to stimuli, calcium signalling dynamics, and the functional relevance of calcium signaling pathways. The findings are compared to previous single-cell studies to draw meaningful conclusions and generate new hypotheses for further investigation and experimentation.

1.5. Intracellular Calcium Signaling

Intracellular calcium plays as a universal second messenger in cells that regulates a vast range of cellular functions, including cell proliferation, muscle contraction, cell death, and neurotransmission. For example, the increase of cytosolic Ca^{2+} concentration or $[Ca^{2+}]_i$ is associated with the activation of G-protein-coupled receptors (GPCRs) which are classified as a cell membrane protein. The GPCRs are considered as the drug targets of 50-60% of therapeutic agents.[65, 66, 66] Cytosolic calcium measurement is one of the most crucial cell-based assays used in new drug candidates screening in the pharmaceutical industry.

Since the 1920s, researchers have made an effort for $[Ca^{2+}]_i$ measurement but few were successful. The first reliable measurements of $[Ca^{2+}]_i$, were performed by injecting the photo protein aequorin into the giant muscle fiber of the barnacle in a study by Ridgway and Ashley. [67] Subsequently, in the 1980s, Tsien and other researchers designed a variety of chemical fluorescent indicators (e.g., Fluo 4 used in this research work) for $[Ca^{2+}]_i$ measurement.[68] Since then, investigations of $[Ca^{2+}]_i$ related intracellular phenomena have increasingly gained interest. Since cytosolic $[Ca^{2+}]_i$ signalling is a time-dependent process regulating diverse cellular processes, real-time measurement is often used to study cytosolic $[Ca^{2+}]_i$ signalling and cellular mechanisms.[69]

1.5.1. Intracellular $[Ca^{2+}]_I$ Homeostasis

The Ca^{2+}-dependent cellular processes are tightly regulated, leading to $[Ca^{2+}]_i$ homeostasis, which refers to the proper distribution of Ca^{2+} ions in cells under resting conditions. For example, under resting or unstimulated conditions, $[Ca^{2+}]_i$ in cells is usually maintained at roughly 100 nM. While extracellular calcium concentration can be as high as ~1.3 mM. The level of cytosolic $[Ca^{2+}]_i$ is determined by a balance between the flux of $[Ca^{2+}]$ into the cytoplasm and the removal of $[Ca^{2+}]$ by the combined actions of channels pumps, and exchangers at any moment. However, cell calcium may be increased or decreased due to various processes. For instance, the processes that can increase $[Ca^{2+}]_i$ include (see Figure 1.7): [70]

1. Ca^{2+} enters a cell from extracellular environment through the plasma membrane largely by different Ca^{2+} channels (i.e., receptor-operated channels, voltage-sensitive channels, store-operated channels).

2. Ca^{2+} enters cytoplasm from the endoplasmic reticulum (ER) through the IP3 and RYR which exist on ER in a process called store-operated calcium entry (SOCE).

3. Ca^{2+} secretion from mitochondria (e.g., as the effect of permeability transition pore (PTP) opening).

4. Ca^{2+} entry via the plasma membrane through the plasma membrane Ca^{2+} ATPase (PMCA) and Na^{+}/Ca^{2+} exchanger (NCX).

The processes that can decrease $[Ca^{2+}]_i$ and release calcium outside a cell, include (see Figure 1.7)

1. Ca^{2+} absorption and uptake by the action of the sarcoplasmic/endoplasmic reticulum Ca^{2+} ATPase (SERCA) pump.

2. Ca^{2+} absorption and uptake by mitochondria through the uniporter inside the cell.

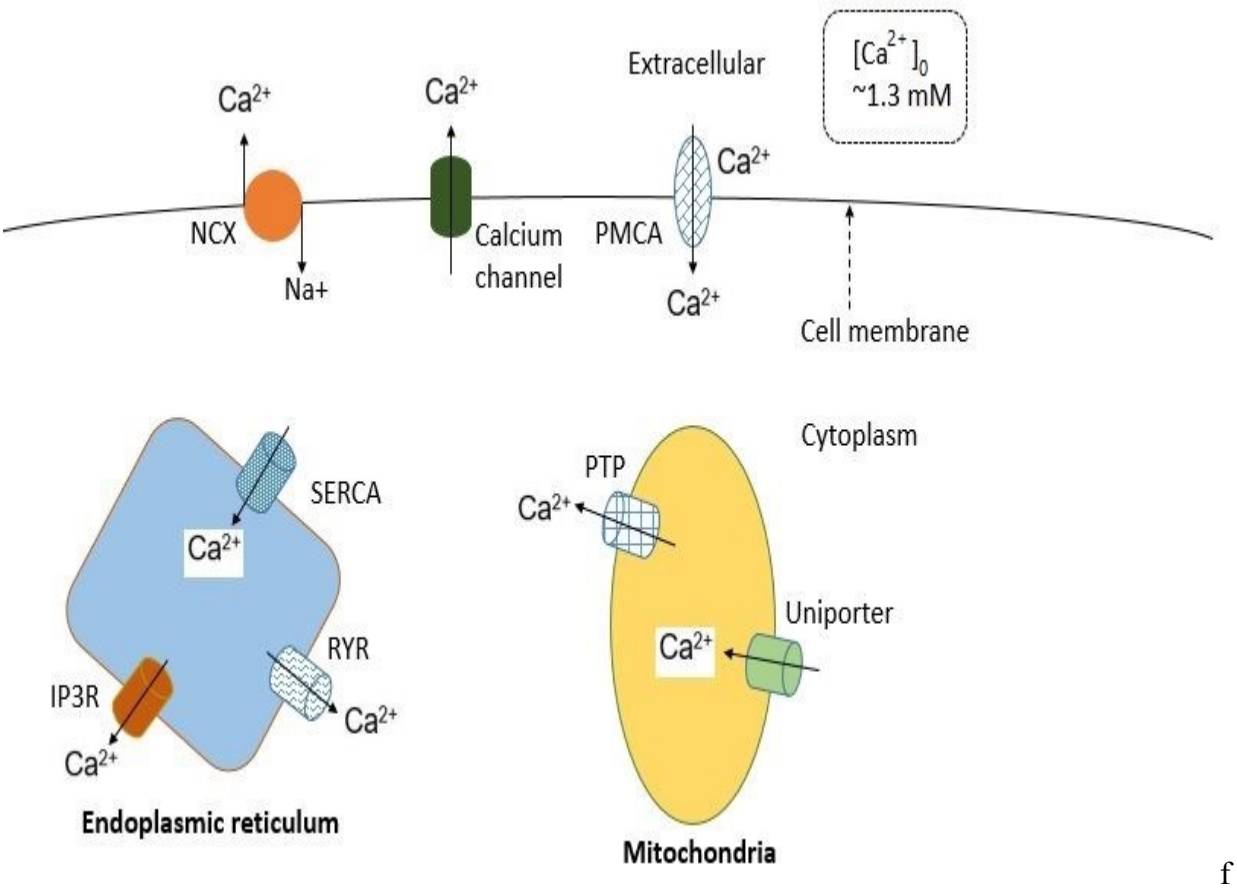

f

Figure 1.7. The increase or decrease of intracellular calcium concentration, which is regulated by various processes.

1.5.2. Changes and Disruption of Ca^{2+} Homeostasis

Alterations of the tightly regulated Ca^{2+} homeostasis can lead to changes in Ca^{2+}, and even cell death. Even non-disruptive alterations in Ca^{2+} signalling could have severe effects on cells. These changes in Ca^{2+} homeostasis can include a sustained increase in cytosolic Ca^{2+}, depletion of ER, or an increase in mitochondrial Ca^{2+}. As an example, the sustained elevation of the cytosolic calcium has been observed to be linked with cytotoxicity and cell death (i.e., apoptosis or necrosis). The cytosolic calcium increase due to stimuli (e.g., anticancer drugs, or other endogenous or exogenous substances) could cause excessive Ca^{2+} to accumulate in mitochondria.[71] This Ca^{2+} overload activates the mitochondrial PTP opening which will result in cell death either via the activation of apoptosis by the release of cytochrome c from

mitochondria into cytosol, [72] or via necrosis. Consequently, it is recognized that the Ca^{2+} increase is an early event leading to cytotoxicity.[73]

Since the $[Ca^{2+}]_i$ increase can be detrimental, single-cell and bulk-cell monitoring of $[Ca^{2+}]_i$ is important. This monitoring has been performed to study the effect of several endogenous and exogenous compounds on different cell lines.

1.5.3. Cytosolic calcium increases by stimulation of G protein coupled receptors (GPCRs)

G protein coupled receptors (GPCR) can detect and bind to ligands outside the cell membrane. About 50% of drugs currently on the market target these families of membrane receptors. [74]Ligands can bind to a GPCR either to transmembrane helices or extracellular N-terminus. After a ligand binds with GPCR, a cellular pathway will be triggered and will cause a specific cellular response (e.g. increase or decrease in cytosolic calcium) to occur. GPCRs can give rise to the intended signal or cellular response (activated) upon binding with an agonist; whereas an antagonist is a ligand that binds to the GPCR and prevents the receptor from producing a cellular response. [75,76]

The structure of GPCR is shown in Figure 1.8. After the ligand (an agonist) binds to the GPCR, its cytoplasmic αq subunit is activated which in turn activates a nearby phospholipase C (PLC) (an enzyme attached to the cell membrane). After its activation, PLC catalyzes the conversion of a phosphatidylinositol 4,5-bisphosphate (PIP2), a phospholipid component of the cell membrane, into inositol trisphosphate (IP3). IP3, which is a soluble molecular messenger, is capable of diffusing through the cytoplasm and binds to IP3-receptor (IP3R) on the surface of the endoplasmic reticulum/sarcoplasmic reticulum (ER/SR), leading to the release of Ca^{2+} from ER/SR into the cytoplasm and elevation of cytosolic calcium concentration according to Figure 1.8 . [77]

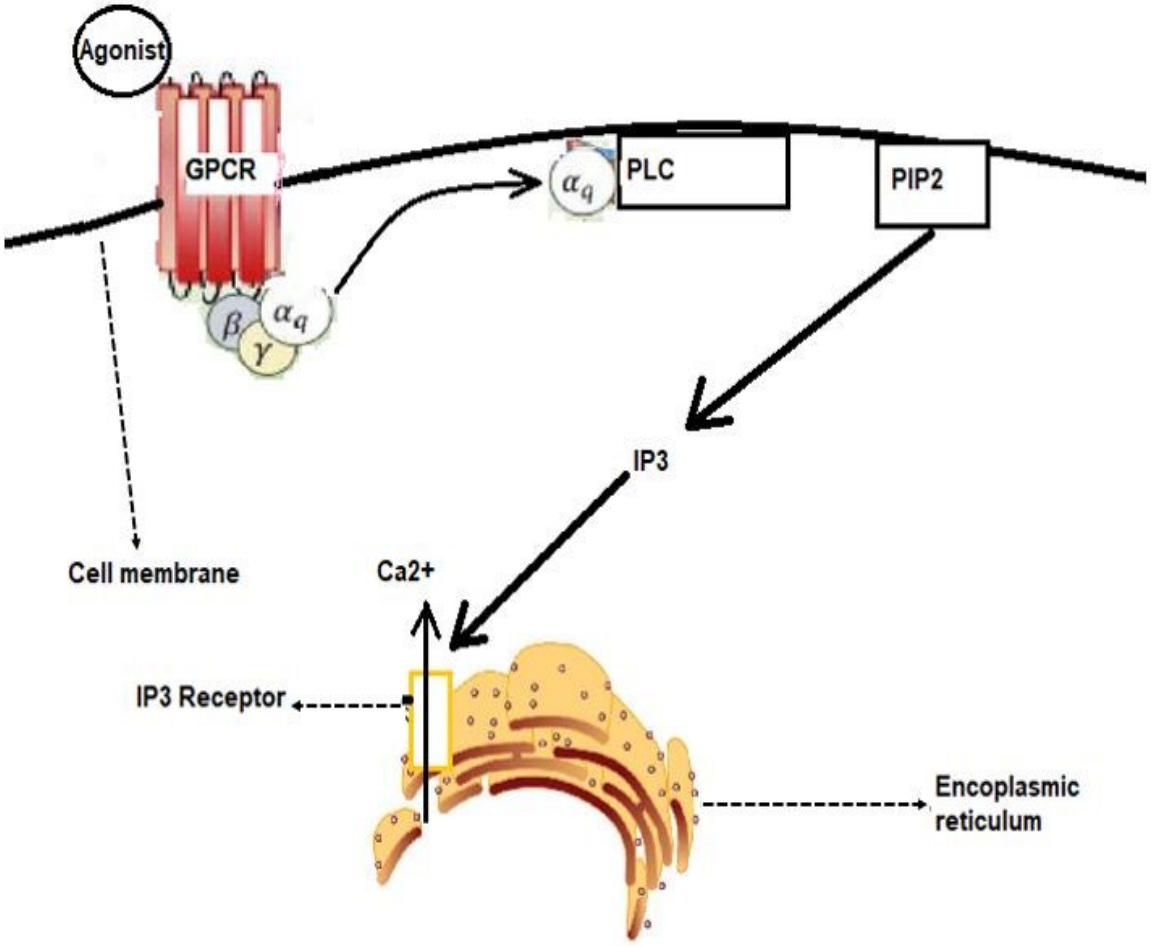

Figure 1.8. Process of activation of GPCR with agonist and subsequent increase in the cytosolic calcium

1.6. Endogenous small molecules overview

Endogenous small molecules are naturally occurring within an organism's cells and tissues. These molecules play crucial roles in various biological processes including signaling, regulation and metabolism, and homeostasis. They are usually produced by enzymatic reactions and are essential for the survival and normal functioning of an organism. [78]

There are diverse sources of endogenous molecules. They can be classified into several categories based on their origin and biosynthetic pathways. Some of the major sources of endogenous small molecules include:

Metabolites: Metabolites are small molecules that are intermediates or end products of metabolic pathways and reactions. These molecules are generated during the decomposition or synthesis of macromolecules such as carbohydrates, lipids, proteins, and nucleic acids. Examples of metabolites are glucose, ATP, NADH, acetyl-CoA, citrate etc.[79]

Hormones: Hormones are chemical messengers that are biosynthesized and secreted by specialized glands or endocrine cells. Hormones regulate different physiological processes, for instance cell growth, metabolism, development, reproduction, and stress response. A few examples of endogenous hormones include Angiotensin I, Angiotensin II and Angiotensin (1-7) which will be further discussed in this thesis.[80] The structure of aforementioned hormones is represented in Figure 1.9.

H_2N-Asp-Arg-Val-Tyr-Ile-His-Pro-Phe-His-Leu-COOH
Angiotensin I

H_2N-Asp-Arg-Val-Tyr-Ile-His-Pro-Phe-COOH
Angiotensin II

H_2N-Asp-Arg-Val-Tyr-Ile-His-Pro-COOH
Angiotensin **(1-7)**

Figure 1.9. Amino acid sequences of Ang I, Ang II and Ang (1-7).

Neurotransmitters: Neurotransmitters are small molecules that expedite communication between neurons in the nervous system. They are released from the presynaptic neurons and bind to postsynaptic neurons' receptors and transmit signals across the synapse. Neurotransmitters include serotonin, dopamine, histamine (Figure 1.10) , acetylcholine, gamma-aminobutyric acid (GABA), and glutamate.[81]

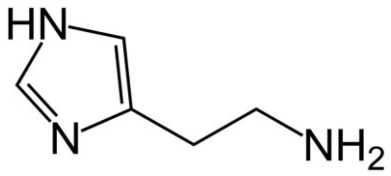

Figure 1.10. Chemical structure of histamine

Signaling Molecules: Signaling molecules also fall in category of endogenous small molecules that regulate cellular processes and pathways. These molecules act as extracellular signaling molecules that mediate communication between cells or as secondary messengers in intracellular signaling cascades. Examples include calcium ions (Ca^{2+}), cyclic AMP (cAMP), cyclic GMP (cGMP), and nitric oxide (NO).[82]

Enzyme-Catalyzed Products: Endogenous small molecules can also exist as products of enzymatic reactions. For example, enzymes, such as cytochrome P450s, which are involved in drug metabolism and detoxification, can produce small molecules as intermediates or by-products during their catalytic activities. [83]

Metabolites of Gut Microbiota: The gut microbiota consists of a diverse community of microorganisms which can metabolize dietary components and produce small molecules with important physiological functions. For instance short-chain fatty acids (SCFAs), such as propionate, acetate, and butyrate are produced by the gut microbiota through the fermentation of dietary fibers and have been implicated in various aspects of host health.[84]

It is important to note that the sources of endogenous small molecules are vast and diverse. The aforementioned examples provide a general overview of the major categories, but there are many other small molecules that contribute to the complexity of biological systems. Understanding the synthesis, regulation, and functions of endogenous small molecules is important for unraveling the intricacies of cellular mechanisms and their effect on overall organismal health. Their study not only improves our understanding of basic biology but also holds potential for developing therapeutic and diagnostic tools for diseases.[85]

1.7. Overview of Exogenous Small Molecules

Exogenous small molecules are chemical compounds that are obtained from external sources and introduced into a living organism. Exogenous small molecules can come from various sources and can have different influence on biological organisms, unlike endogenous small molecules which are naturally produced within the organism. They can enter the living organism through environmental exposure, dietary sources or deliberate administration for therapeutic purposes. Understanding the definition and different sources of exogenous small molecules is crucial for studying their impact on biological processes and their potential applications in research and medicine.[86]

Exogenous small molecules can be introduced to our body from the food we consume. Plants and animals have a variety of small molecules such as vitamins, phytochemicals, and flavor compounds. For instance, antioxidants like vitamins C and E, as well as phytochemicals like flavonoids and carotenoids, are commonly found in vegetables, herbs and fruits. [87]

Nutritional supplements such as vitamins, minerals, amino acids, and herbal extracts are manufactured to provide extra exogenous small molecules to support overall health and well-being. These supplements are usually taken in the form of capsules, pills, or powders. [87]

Airborne Substances: Exogenous small molecules can be inhaled from the environment. Air pollutants, for example, particulate matter, volatile organic compounds (VOCs), and toxic gases, introduces exogenous small molecules into the respiratory tract and system. Pollutants from vehicle exhaust, industrial emissions, and cigarette smoke are a few examples.[88]

Water waste may have exogenous small molecules such as pesticides, pharmaceutical residues, and disinfection byproducts. These water contaminants, through drinking water or aquatic exposure, may enter the body.[89]

Therapeutic agents, which include a vast range of exogenous small molecules utilized in medical treatments, are biologics, monoclonal antibodies, peptides, and gene therapeutics. These substances are designed for targeted interventions in particular diseases or conditions.[90]

Medications: Pharmaceuticals are exogenous small molecules which are designed and formulated for specific therapeutic purposes. These substances include over-the-counter drugs and prescription medications used to treat different medical conditions. For example antibiotics,

antihypertensives, analgesics, and anticancer drugs are among the pharmaceuticals and therapeutics.[91]

Occupational Exposures: Workers in some industries may contact exogenous small molecules during their job duties. Exposure to chemicals, solvents, heavy metals, and other toxic substances happens in in the workplace. Industrial workers, laboratory personnel, and agricultural workers who handle pesticides or fertilizers can be exposed to these chemicals.[92]

Exogenous small molecules can be present in different industrial products such as cleaning agents, paints, plastics, and cosmetics. These products may release volatile gases or have constituents that can be absorbed through the skin or by inhalation.[93]

Recreational Substances: Exogenous small molecules can be found in recreational substances, including cannabinoids, alcohol, and tobacco. These chemical substances contain psychoactive compounds with profound effects on the central nervous system and overall health.[94] Figure 1.11 illustrates the chemical formula of cannabinoid compounds that are included in exogenous small molecules category and will be studied in chapter 3 of this thesis.

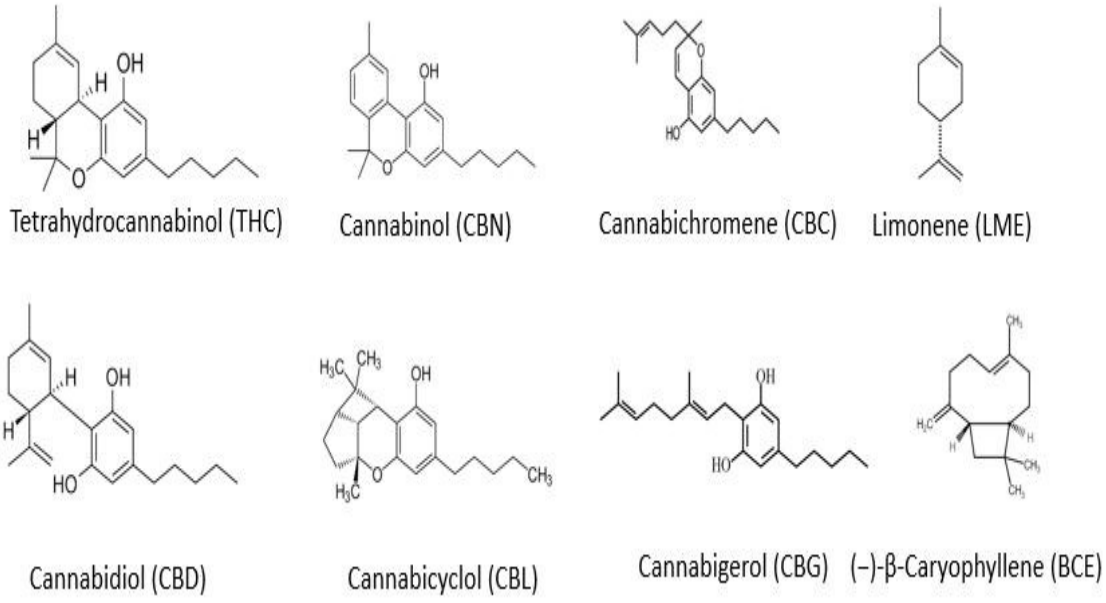

Figure 1.11. Chemical structures of THC, CBN, CBC,LME,CBD, CBL, CBG, BCE.

Understanding the sources of exogenous small molecules is crucial for studying their impact on biological systems, for identifying potential risks or benefits, and for developing safe and effective usage strategies. Scientists can obtain insights into their roles in human health, disease, and environmental interactions by considering the origins and impacts of exogenous small molecules.

1.8. Histamine overview and histamine related intracellular calcium signaling

Histamine is a neurotransmitter which is biosynthesized in the body by the decarboxylation of histidine which is an essential amino acid found in many foods. Histamine is stored in specialized cells, mast cells, which are found in tissues all over the body and will be released to other tissues upon simulation by an allergen or other irritant which can eventually lead to an inflammatory response. [95, 96]

In the digestive system, histamine regulates the secretion of gastric acid. Furthermore, histamine is involved in the inflammatory response by stimulating the production and secretion of cytokines and other immune system mediators. Histamine also contributes to the

pathogenesis of certain autoimmune diseases, for example multiple sclerosis and rheumatoid arthritis. [97, 98] Histamine also has a role in the regulation of sleep-wake cycles, body temperature, blood pressure, and heart rate.[99]

A549 cells, both wild type and ACE2-enriched ones, are a human alveolar epithelial cell line obtained from lung adenocarcinoma.[100] Histamine can interact with the A549 cells through histamine receptors, namely H1, H2, H3, and H4.[101] All the histamine receptors are subtypes of GPCRs (G protein-coupled receptors) which will produce cytosolic calcium increase upon activation.[82] H1 and H2 receptors are more abundant compared to H3 and H4.[102] Activation of H1 receptors on A549 cell surface can stimulate the production of pro-inflammatory cytokines, e.g. interleukin 6 (IL-6), IL-8, and tumor necrosis factor alpha (TNF-α), and can in turn activate the IP3 pathway and increase cytosolic calcium concentration.[103] Overproduction of these cytokines can trigger lung inflammation and injury. Instead, activation of H2 receptors increases the level of cyclic adenosine monophosphate (cAMP), which is a derivative of adenosine triphosphate (ATP), and induces the production of anti-inflammatory cytokines such as IL-10. [104] H2 receptor also intervenes in gastric acid secretion from parietal cells in the stomach. H3R, H4R have not been studied well but these receptors attracted attention as a novel target to modulate various histamine-mediated immunologic and inflammatory disorders such as cancer and autoimmune disease.[101] Figure 1.12 represents the function of different histamine

receptors.

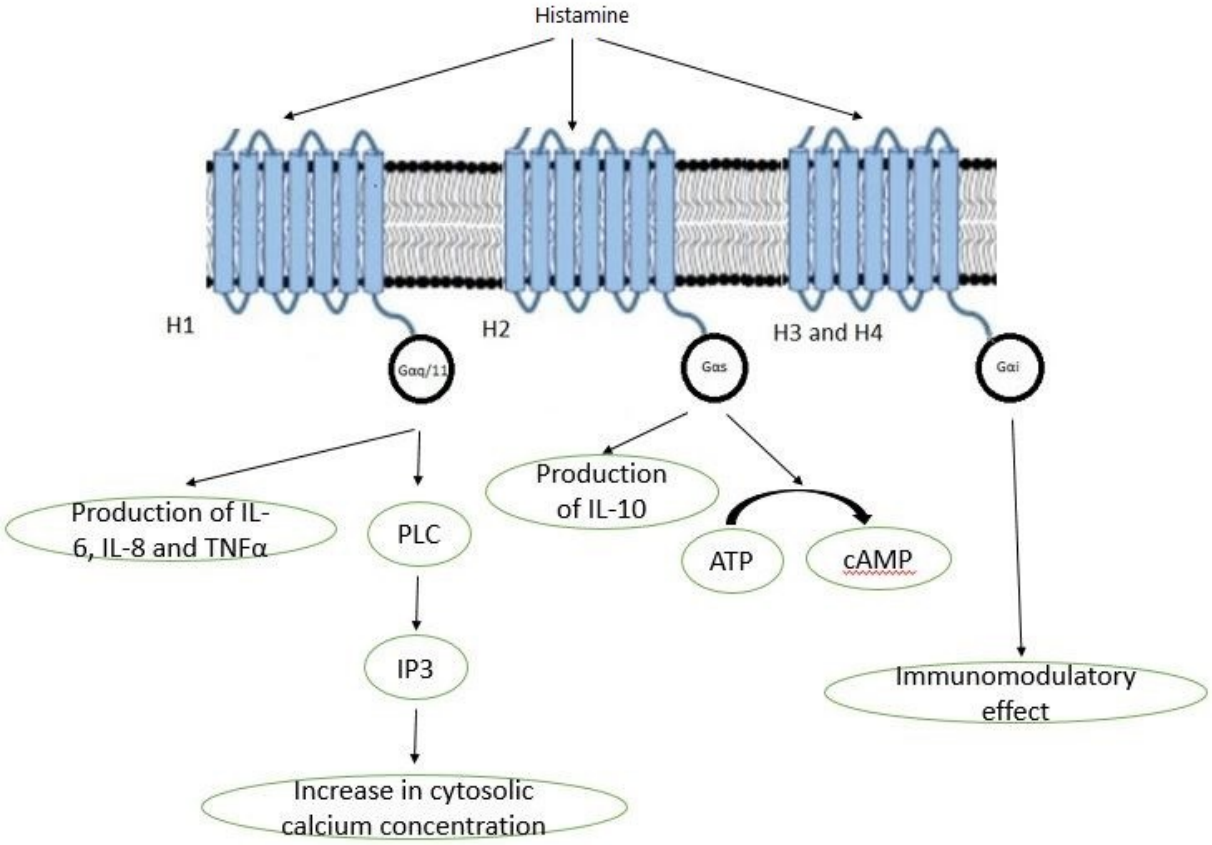

Figure 1.12. Occurrence of different histamine receptors and their cellular responses

Histamine can also regulate the function of other cell types in the lung such as immune cells and fibroblasts. For instance, histamine can trigger the migration of neutrophils and eosinophils (two types of immune cells) to the lung. These cells can lead to secretion of various inflammatory mediators that can affect lung cells. Histamine can also stimulate the activation of fibroblasts and can contribute to the development of fibrotic lung diseases. [105]

A549 cells express both H1 and H2 histamine receptors and their response to histamine has been studied extensively.[102] The activation of H1 receptors in A549 cells will increase cytosolic calcium concentration. This increase in $[Ca^{2+}]_i$ in endothelial cells can be measured with fluorescent calcium indicator dyes, such as Fura-2 or Fluo-4. [106]

In one study, A549 cells were stimulated with histamine, and the results showed that histamine induced an increase in $[Ca^{2+}]_i$, which first peaked by the stimulation and then slowly

reduced and returned to its normal concentration.[88] The increase in cytosolic calcium concentration was obstructed by the H1 receptor antagonist mepyramine.[107] These results illustrate that this block in cytosolic calcium concentration is mediated by H1 receptors.[108] Studies also illustrate that histamine-induced calcium signalling was dependent on extracellular calcium since the removal of extracellular calcium eliminates the response. [109, 110, 111]

1.9. Angiotensin (1-7) overview and angiotensin related cytosolic calcium signaling

Angiotensin is an essential polypeptide and one of the components of the human renin-angiotensin system (RAS). RAS is a blood pressure and fluid balance regulatory system in the human body. RAS is a sophisticated system that produces several peptide hormones, including renin, angiotensin I (Ang I), angiotensin II (Ang II), and angiotensin (1-7). [112] In the following paragraphs, the production, metabolism, and physiological effects of these hormones will be elaborated on.

Angiotensin is produced in several steps and processes with the action of different enzymes. The first step in the production of angiotensin is the release of renin from kidney cells. Renin is an enzyme that splits angiotensin, which is a protein produced by the liver, to produce Ang I. Ang I is subsequently converted to Ang II by angiotensin-converting enzyme (ACE). ACE is also a protein receptor located in the lungs, heart, brain, and kidneys (see Figure 1.13). [113]

ACE is a zinc metallopeptidase that removes two amino acids from the carboxyl-terminal of Ang I (a decapeptide) to produce Ang II (an octapeptide). Ang II causes constriction of blood vessels (vasoconstriction) which can increase blood pressure. On the other hand, Ang II can be cleaved by other enzymes such as angiotensin-converting enzyme 2 (ACE2) to produce angiotensin (1-7). Ang (1-7) is a vasodilator, and its function is contrary to the vasoconstrictive effects of Ang II. [114]

The physiological effects of Ang II are regulated by its interaction with cell membrane receptors. Angiotensin type 1 (AT1) and angiotensin type 2 (AT2) receptors are among the aforementioned receptors. [113]

AT1 receptors are found in the kidneys, cardiovascular system, and brain. Activation of AT1 by Ang II results in vasoconstriction (an increase in blood pressure and fluid volume). In

addition to the vasoconstriction effects, Ang II has other physiological effects, including effects on inflammation, cell growth, and oxidative stress. AT2 receptors are less studied compared to AT1 receptors and are found in certain areas of the brain. Unlike the AT1 receptor, the activation of AT2 receptors by Ang II leads to vasodilation and anti-inflammatory effects.[115]

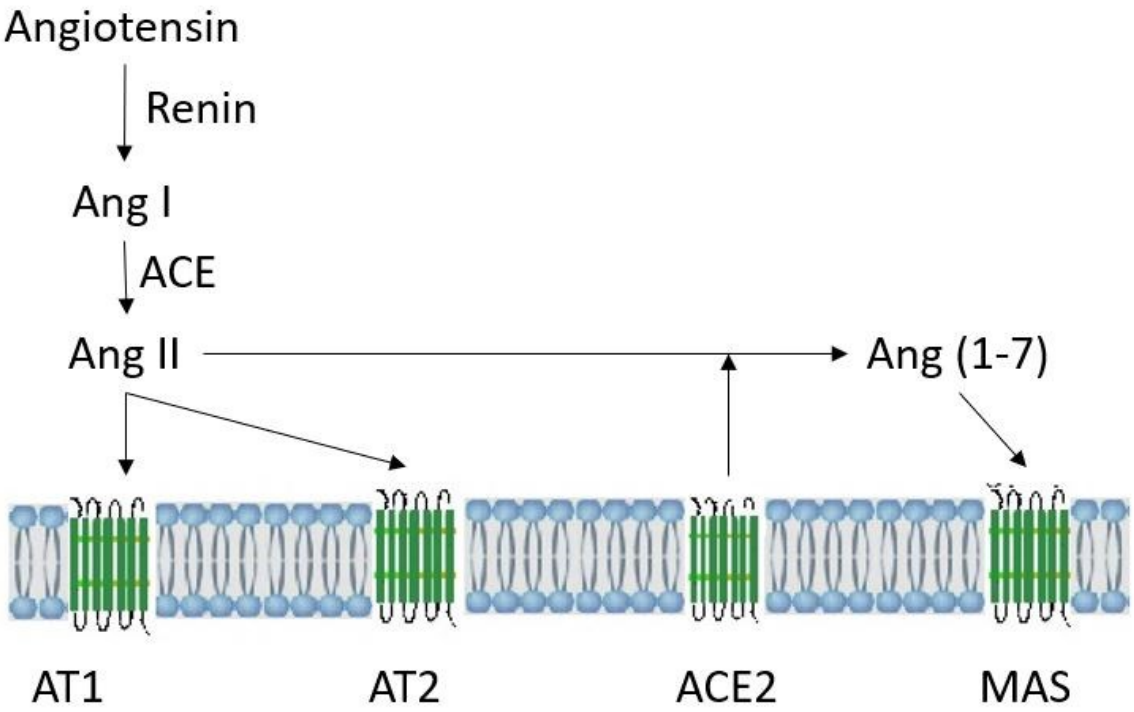

Figure 1.13. Membrane receptors and polypeptides in the renin-angiotensin system (RAS). Membrane receptors include ACE, ACE2, AT1, AT2 and MAS. Polypeptides include angiotensin, Ang I, Ang II, Ang (1-7).

1.9.1. Ang (1-7) effect on activation of MAS receptor and the COVID-19 disease:

COVID-19 is caused by the virus named severe acute respiratory syndrome corona virus 2 (SARS-CoV-2) entering the host cells, initially in the airways, mouth, eyes, and lungs. This virus caused COVID-19 pandemic which was lasting for several years and caused millions of deaths and acute social and economic consequences.[115] The SARS-CoV-2 spike protein can attach to one or more proteins that are expressed in these tissues' cell membranes at varying levels, allowing the virus to enter the cell and get multiplied. [116] A number of proteins have been identified as potential SARS-CoV-2 binding partners, including extracellular matrix

metalloproteinase inducer or CD147 [117], sialic acid receptors, transmembrane serine protease 2, angiotensin converting enzyme 2 (ACE2), and transmembrane serine protease 2 . Among these, alveolar epithelial type II cells and airway cells exhibit the highest levels of ACE2 expression. [118]

The loss of ACE2 from the cell membrane, as a result of SARS-CoV-2 binding, is a significant contributor to the progression of the COVID-19 disease according to Figure 1.14. Renin-angiotensin system (RAS) enzyme ACE2 converts angiotensin (Ang) II to Ang-(1-7) with high affinity. [119] With very few exceptions, a reduction in ACE2 cell membrane availability will change the balance of the RAS in the lungs, blood vessels, and circulation towards an increase in Ang II and a decrease in Ang-(1-7). According to experimental and clinical data, Ang-(1-7)/Mas receptor axis activation is a significant axis and defence mechanism against the harmful effects brought on by an unwarranted rise in Ang II/AT1 receptor in several disorders. Accordingly, stimulation of the MAS receptor or injection of Ang-(1-7) or MAS analogues can be additional approaches to reduce the inflammatory response mediated by SARS-CoV-2. [120, 121] The possible activation of MAS receptor by Ang-(1-7) which is a GPCR and resulting elevation in cytosolic calcium concentration is one of the main interest of this thesis. Furthermore, blockage of the ACE2 receptor that might reduce the cytosolic calcium concentration by loss of function of ACE2 in RAS system can also be monitored by cell calcium measurement techniques.

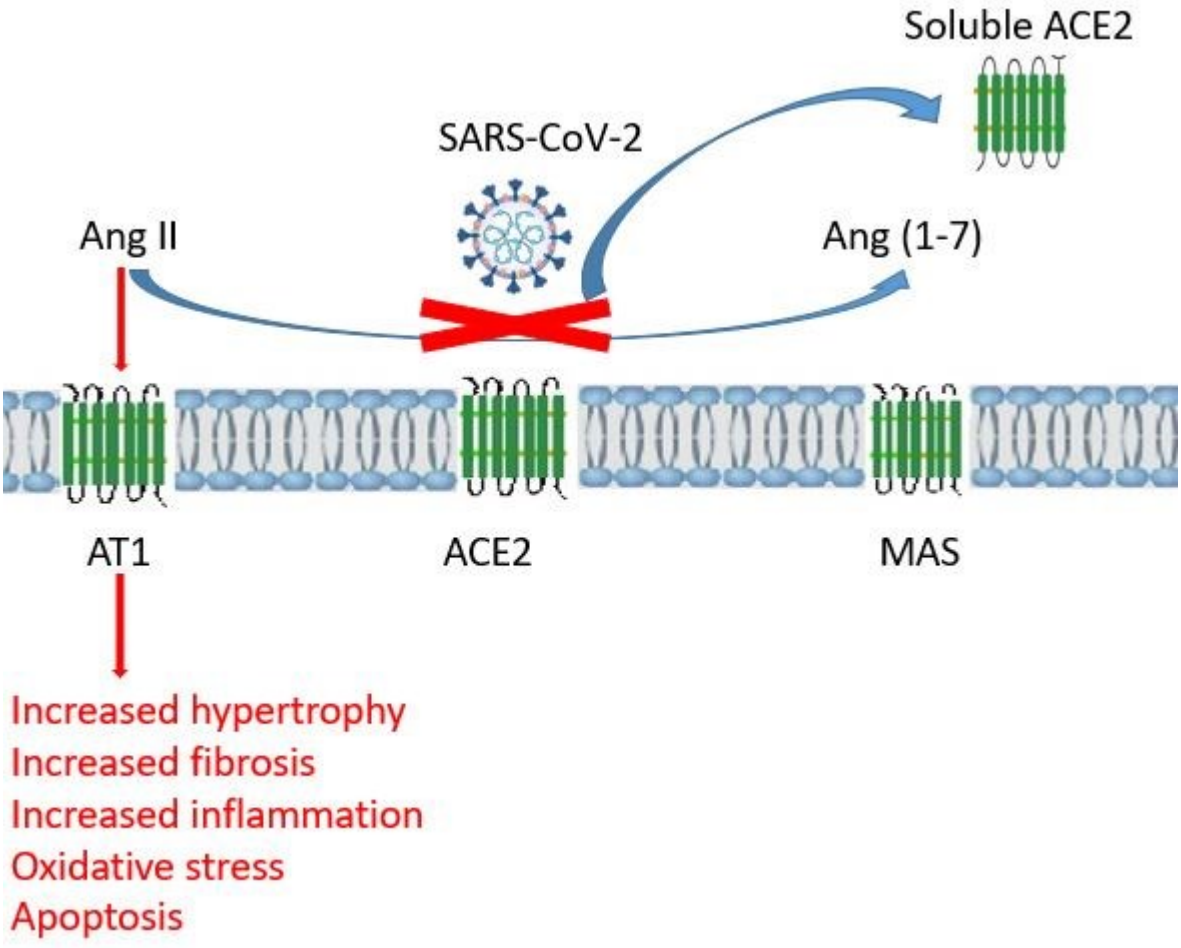

Figure 1.14. Disruption of RAS system caused by the SARS-CoV-2 (sever acute respiratory syndrome corona virus 2).

Activation of MAS receptor has been proposed in several studies to treat COVID-19, and therefore the study of cytosolic calcium concentration and MAS activation can be highly relevant. [122]

1.9.2. Ang (1-7) effect on cancer

Ang (1-7) can be implicated in other diseases such as brain cancer as a treatment. The Mas receptor (MASR), a G protein-coupled receptor that is expressed in various tissues i.e. brain, is activated by Ang(1-7). [113] The U-87 MG (human glioblastoma) cell line is used as a model to study pharmacology. Recent studies have shown that U-87 MG cells express MASR

and can be activated by Ang (1-7) stimulation. In the following paragraph, relationship between U-87 MG cells and Ang (1-7), including its effects on proliferation, migration, and invasion will be elaborated. [123, 124]

1.9.3. Expression of MASR in U-87 MG Cells:

Several studies have claimed the expression of MASR in different human cancer cell lines and brain tissues. Burghi et.al (2012) claimed that brain cells express MASR at both the mRNA and protein levels. Since U87 MG cells are also brain tissue cells the high MASR expression in these cells is probable.[125]

1.9.4. Ang(1-7) effect on cytosolic calcium concentration:

Many papers reported an increase in cytosolic calcium concentration by stimulation with Ang(1-7) in cancer cells such as MDCK.[126] In a report by Burghi et.al, the increase in cytosolic calcium concentration was not observed either in wild type A549 cells or in MAS-transfected A549 cells.[127]

In previous studies, it's been observed that the activation of the MAS receptor in A549 wild type cells and MAS transfected A549 cells with Ang(1-7), will not elevate cytosolic calcium concentration. In this study, Fura 2 was used as a fluorescent dye and the experiment was performed using bulk-cell measurement techniques. On the other hand, a positive experiment with histamine showed an increase in cytosolic calcium concentration according to Figure 1.15.[127] However, this study wasn't performed on a single cell biochip and the study didn't have any information about effect of Ang(1-7) on other cell lines such as U87 MG.

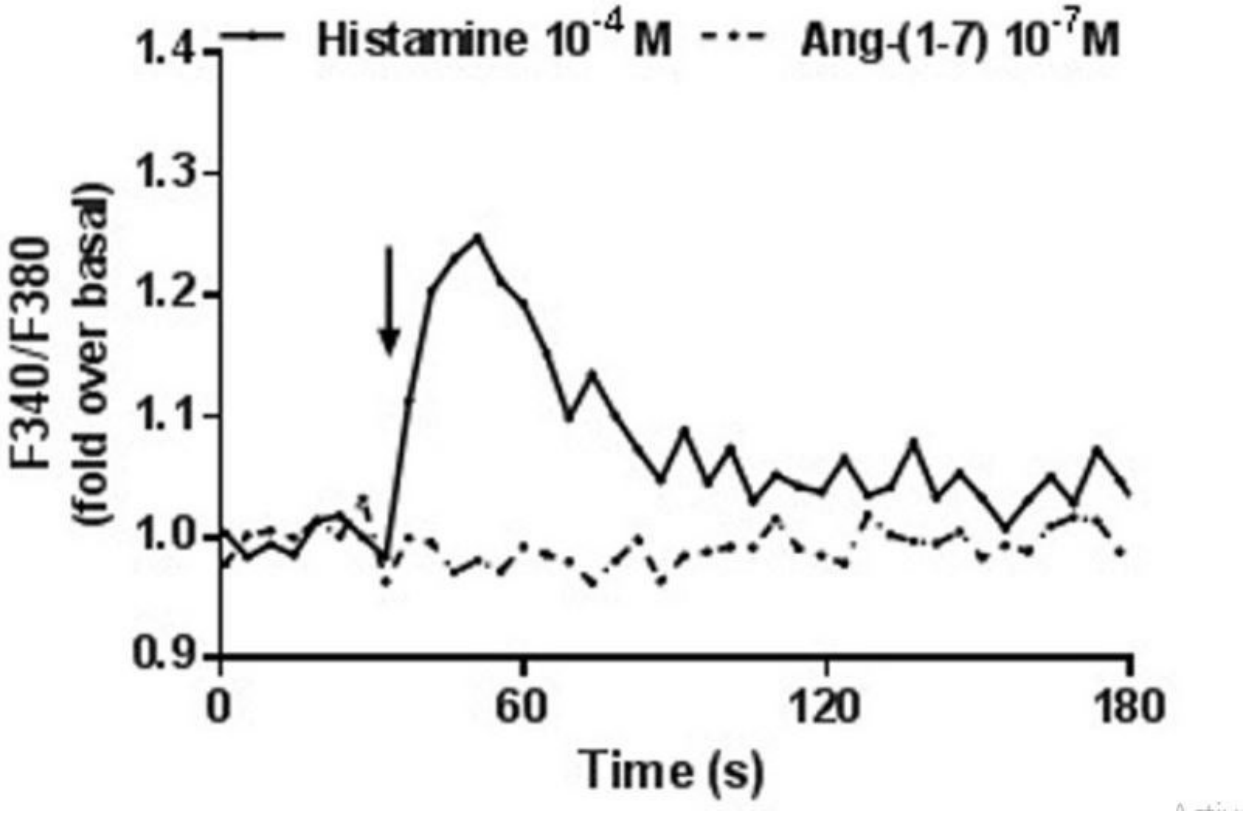

Figure 1.15. Intracellular Ca2+ concentration in response to Ang-(1–7) and histamine in MAS transfected A549 cells. [127]Reprinted with permission from the Frontiers in Pharmacology.

1.10. Research objectives:

The primary goal of this research is to compare single-cell and bulk-cell calcium measurement methods, thereby providing a better understanding of cellular calcium signaling dynamics. By integrating these two methodologies, there are three research objectives described as follows.

1.10.1. To characterize cell-specific responses of exogenous and endogenous compounds:

We will explore the sophisticated calcium response patterns at the single-cell level, in order to enable researchers to identify and characterize cell-specific behaviours in response to various stimuli due to endogenous and exogenous sources.

1.10.2. To reveal population-wide trends on A549 and U-87 MG cells:

Simultaneously, we will gain insights into cell heterogeneity within a cell population by utilizing bulk-cell calcium measurements. Bulk-cell calcium measurements will enable the identification of collective cellular responses and their impact on calcium signaling patterns.

1.10.3. To advance calcium signaling modulation on U-87 MG cells:

We will investigate the potential modulation of calcium signaling by measuring the effects of histamine, cannabinoids (CBD, CBN, CBC, CBL, CBG), and terpenes (BCE, LME, MYR) on cytosolic calcium concentration. This exploration aims to study the regulation of intracellular calcium dynamics.

By pursuing these objectives, our research goal is to enhance our knowledge about calcium signaling dynamics, potentially paving the road for innovative interventions in various fields, including biology and medicine. Ultimately, the integration of single-cell and bulk-cell approaches expands our understanding of cellular responses and signaling pathways, offering exciting possibilities for scientific achievements and improved healthcare outcomes. Schematic diagram of the contents in this thesis is illustrated in Figure 1.16.

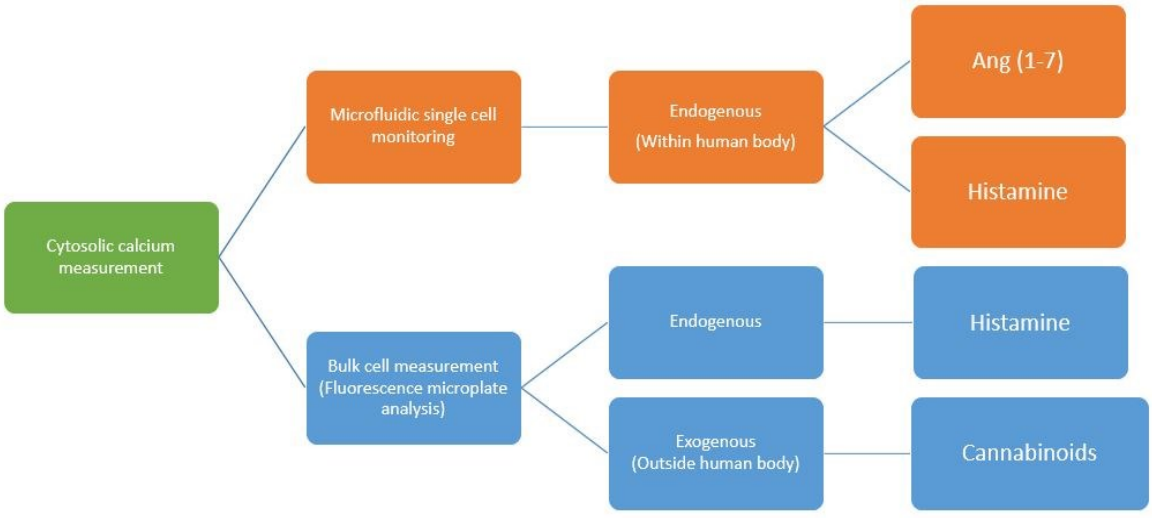

Figure 1.16. Table of contents

Chapter 2. Methodology

2.1. Cell culture

2.1.1. U-87 and wild type A549 cell thawing and cell culture procedure

2.1.1.1 Thawing cells

1. The cryo-glove (blue glove as shown in Figure 2.1a) and a styrofoam box containing ice were taken. Wash medium (no serum) and culture medium (with FBS) were prepared. The CO_2 cell incubator was assured to operate properly.

2. The cryo-glove was used to remove a tower from the liquid nitrogen (LN2) tank (Figure 2.1a); the tower was placed on the bench (Figure 2.1b); the long safety pin was carefully removed; a cell box (Figure 2.1c) was removed; a cryotube vial was taken and the label and place the vial in a styrofoam box on the bench.

3. The box was carefully replaced in the tower, the safety pin was put back, and ensure that the tower is always faced upward when handling, and the tower is put back into the LN2 tank.

4. The cryotube vial, which consisted of 1 mL of cryopreserved cells, was taken out from the styrofoam box, and the vial was put into a water bath at room temperature.

5. The outside of the cryotube vials was dried off, and they were sprayed with a 75% ethanol solution before being placed in the biosafety cabinet.

6. In a 15-mL centrifuge tube, 9 ml of wash medium (no serum) was added to 1 mL of cryopreserved cells; the cell suspension was centrifuged down to produce a cell pellet, and the supernatant was removed.

7. The cell pellet was resuspended by adding 9 mL of culture medium (with FBS) to it; the cells were pipetted up and down, and the cell suspension was put in a culture plate or flask and kept in the incubator.

8. The cells were checked for adhesion inside the flask after 24 hours (Figure 2.2a). If the cells did not attach, 4-5 mL of fresh culture medium was added.

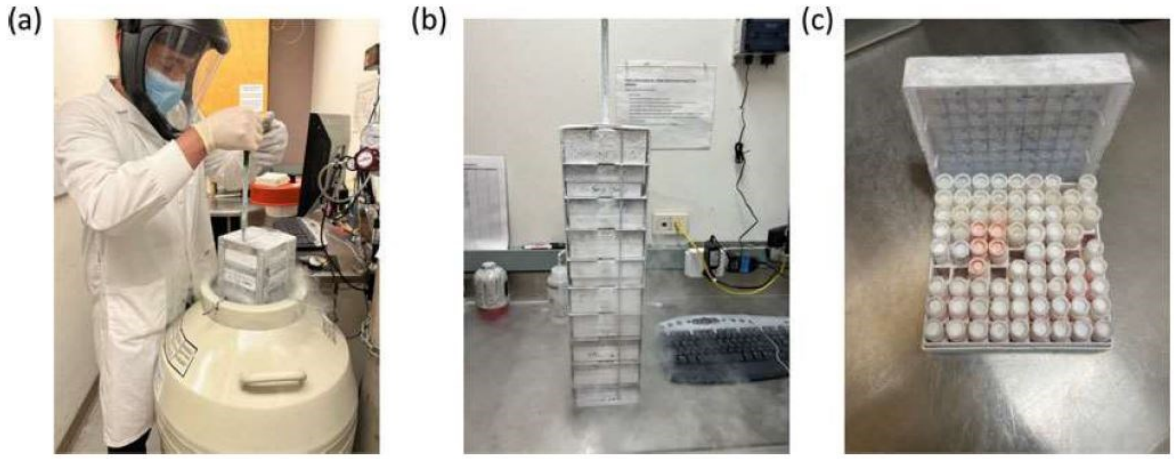

Figure 2.1. Cryovials placed in towers stored in a LN2 tank; A) a tower secured with the long safety pin being taken out of the tank , B) a tower with a handle on top and with a safety pin securing the boxes, C) a box opened to show labeled cryovials.[127]

2.1.1.2. Sub-culturing (passaging) cells

1. Adherent cells were checked under the microscope. The confluency of the cells was required to be more than 80% (Figure 2.2). The cell culture plate was removed from the incubator.

2. Culture medium was removed from the cell culture plate.

3. The cell layer was briefly rinsed with 1mL PBS obtained from the Thermo Fisher Scientific solution to eliminate all traces of serum containing trypsin inhibitor.

4. A suitable amount of Trypsin-EDTA obtained from the Thermo Fisher Scientific (usually 2-3 mL) solution was added to the flask, and the cells were observed under the microscope after 5 to 15 minutes until the cell layer was dispersed.

5. The cell and trypsin suspension were transferred into a centrifuge tube. The plate was rinsed with 2mL of complete growth medium (with FBS) or pure FBS, and the liquid was transferred into the centrifuge tube. This step was repeated twice. The tube was centrifuged. The correct centrifugation time and force for the cell line were checked on the ATCC website.

6. After centrifugation, a cell pellet could be seen at the bottom of the centrifuge tube. The supernatant was carefully removed without disturbing or removing the cell plate. Subsequently, 1 mL of complete growth medium was added to the centrifuge tube, and the cells were pipetted up and down. Immediately, 0.5 mL of the cell suspension was separated for the microfluidic experiment. The rest of the liquid was transferred into a new plate, and 9 mL of growth media was added to the plate.

7. The name of the cell line, passage date, passage number, and name of the lab were written on the cell plate. The cell plate was incubated at 37°C.

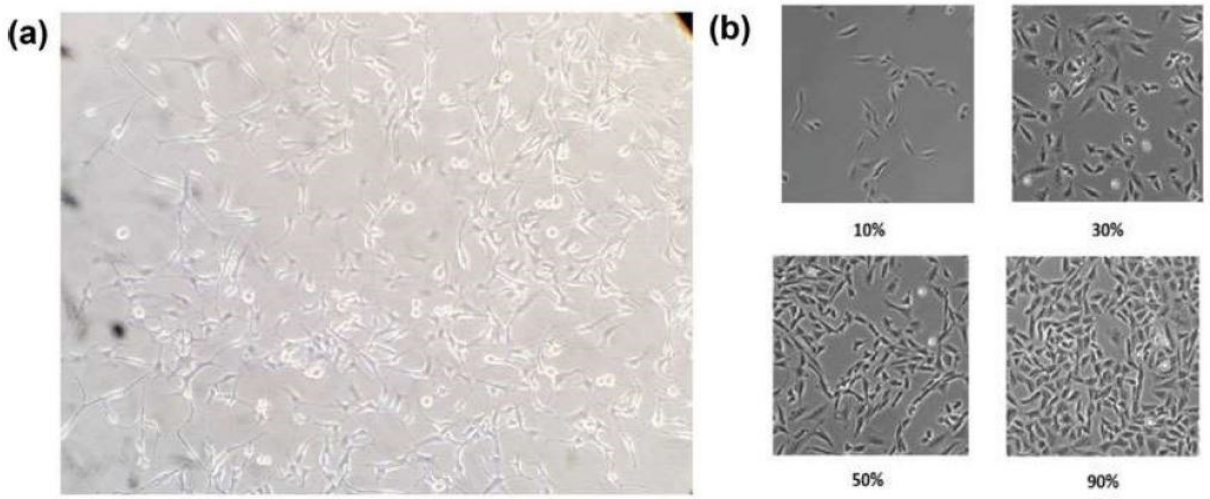

Figure 2.2. Culture of adherent cells; A) adherent cells (star-shaped) and detached cells (round) B) Confluency estimation guide.[128]

2.1.2. ACE-overexpressing A549 cell culture procedure

A549-hACE2 cell line, which is a commonly used cellular model for the study of respiratory infections, has been generated from the A549 lung carcinoma cell line. [100] A549-hACE2 cells were stably transfected to express the human ACE2 (hACE2) gene, Therefore, in contrary to their parental cell line, they are permissive to infection by SARS-CoV-2 and/or spike-pseudotyped lentiviral particles. Accordingly, the cells are ideal for studying the SARS-CoV-2 Spike protein, viral entry into host cells, as well as for screening small molecule inhibitors and neutralizing antibodies. [129]

The additional expression of the human TMPRSS2 gene in the A549-hACE2-TMPRSS2 cells significantly increases their susceptibility to SARS-CoV-2 infection than A549-hACE2.[122]

2.1.3. General cell handling procedures

2.1.3.1 Required Cell Culture Medium

Growth Medium: DMEM, 4.5 g/l glucose, 2 mM L-glutamine. 10% heat-inactivated fetal bovine serum (FBS; 30 min at 56 °C). Penicillin-Streptomycin obtained from Thermo Fisher Scientific (100 U/ml-100 ug/ml). Required Selection Antibiotic: Puromycin

Medium for freezing cells: DMEM, 4.5 g/l glucose, 10% FBS, 10% DMSO

2.1.3.1 Initial Culture Procedure

1. The vial was thawed by gentle agitation in a 37 °C water bath. To reduce the possibility of contamination, the vial's O-ring and cap were kept out of the water. Thawing was rapid (approximately 2 minutes).

2. The vial was removed from the water bath as soon as the contents were thawed and decontaminated by dipping in or spraying with 70% ethanol.

Note: All of the steps from this point should be carried out under strict aseptic conditions.

3. Cells were transferred to a larger tube containing 15 mL of pre-warmed growth medium. Selection antibiotics were not added until the cells had been passaged twice.

4. The tube was centrifuged at 200-300 g for 5 minutes.

5. The supernatant containing the cryoprotective agent was removed, and cells were re-suspended with 1 mL of growth medium without selective antibiotics.

6. The contents were transferred to a T-25 tissue culture flask containing 5 mL of growth medium without selective antibiotics.

7. The culture was placed at 37°C in 5% CO2.

2.1.3.2 Frozen Stock Preparation

1. Cells were re-suspended at a density of 5-7x 10^6 cells/mL in freshly prepared freezing medium.

Note: A T-75 culture flask typically yields enough cells for preparing 1-2 frozen vials.

2. 1 mL of cell suspension was dispensed into cryogenic vials.

3. Vials were placed in a freezing container and stored at -80°C overnight.

4. Vials were transferred to liquid nitrogen for long-term storage.

2.1.3.3 Cell maintenance:

1. Adherent cells were grown as A549-hACE2 cells. To detach cells, the cell layer was rinsed with PBS, and then it was incubated with 0.25% trypsin-EDTA for 2-5 minutes.

2. After ensuring that cell growth is well, (after at least 2 passages), the cells were maintained and subcultured in growth medium supplemented with 0.5 µg/mL of Puromycin.

3. Growth medium was renewed twice a week.

4. Cells were passaged when a 70-80% confluency was reached. The cells were not allowed to grow to 100% confluency.

Note: The average doubling time for the A549-hACE2 cells is 25 hours using the conditions described above

2.2. Single cell cytosolic calcium measurement procedure utilizing a microfluidic chip

2.2.1. Chip fabrication:

1. A glass chip containing three reservoirs, three channels, and one chamber was designed, as shown in Figure 2.3a[130]

The chip can be fabricated by standard chip cleaning, thin film deposition, photolithography, photoresist development, hydrofluoric acid wet etching, reservoir forming, and chip bonding.[130] Similar to a previously reported paper, this chip includes a chamber that contains a V-shaped cell retention structure for single-cell isolation, see Figures 2.3.a and 2.3.c.

2.2.2. Microscopic system

1. An optical system consisting of an inverted microscope (TE300, Nikon) and a CCD camera for bright-field imaging was used, as shown in Figure 2.3.b.

2. A TV monitor was used for easy and clear microscopic observation. For image capture, a video capture card was used, which had been installed in a computer.

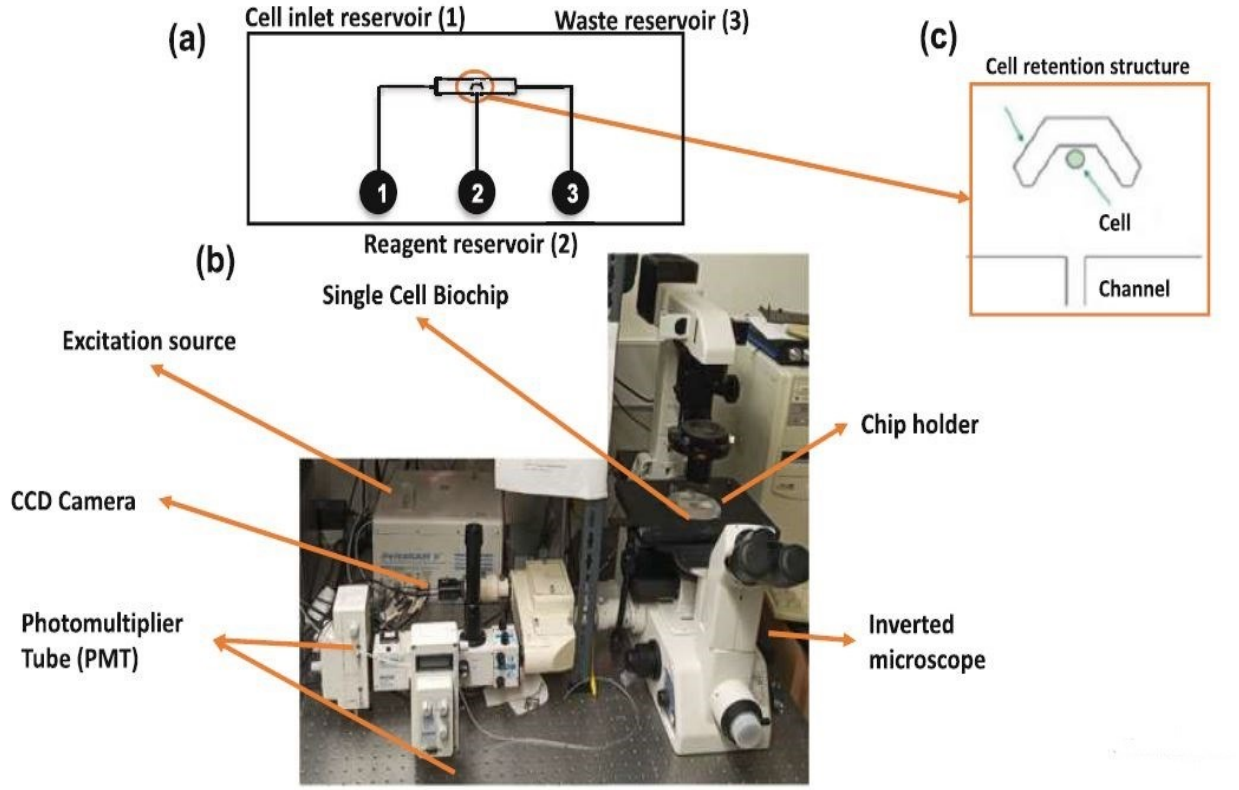

Figure 2.3. The microfluidic chip and the imaging/measurement system. (a) The schematic diagram of the microfluidic chip consisting of three solution reservoirs and cell retention structure. (b) An image of the instrument setup that consist of an inverted inverted microscope, chip holder, excitation source, CCD camera, and PMT. (c) A single (U-87 MG) cell is retained in the cell retention structure that is opposite to the reagent channel leading to the chamber.[128]

2.2.3. Optical imaging & fluorescence measurement

1. A xenon arc lamp coupled with a monochromator was used for dye excitation, as seen in Figure 2.3b.

2. A dichroic filter (620 nm) was used to allow only the red light to enter the video camera for cell imaging, while permitting the green fluorescent emission to reach the microphotometer system, consisting of the photomultiplier tube (PMT) through a detection aperture.

3. The data were acquired using the Felix software. The data were downloaded as an ASCII file for analysis.

2.2.4. Single cell selection and retention in a microfluidic biochip

The first step of single-cell analysis was to select a single live and healthy cell from a cell suspension. Subsequently, the single cell had to be retained in a specific location inside the chip within the observation region defined by the detection aperture during the experiment. Due to the adherent nature of glioma cells, the cells were attached to the V-shaped cell retention structure after incubation for ten minutes. This cell retention provided the opportunity for the measurement of the change in intracellular calcium concentrations during the delivery of reagents.

2.2.5. Washing and priming the biochip

1. The microfluidic chip was placed onto the microscope stage, and the focus knob was adjusted until the cell retention structure was clearly visible. It was ensured that the microphotometer was set to "View" (see appendix A, note 7).

2. An aliquot (5 µL) of 70% ethanol was added to Reservoir 1, and the liquid was allowed to fill and prime the channels. Care was taken to ensure that there were no air bubbles in all channels and the chamber. Ethanol from Reservoir 1 was removed by gentle suction (see appendix A, note 8).

3. Aliquots (5 µL) of 70% ethanol were added to Reservoirs 1 and 2. All channels and the chamber were examined for air bubbles, and ethanol was removed via Reservoir 2, then Reservoir 1 (see appendix A, note 9).

4. An aliquot (5 µL) of cell medium solution was added to Reservoir 2 and then Reservoir 1. All channels and the chamber were checked for any air bubbles, and the medium solution was discarded via Reservoir 2 and then Reservoir 1.

5. Step 4 was repeated two times.

6. An aliquot of 5 µL of cell medium solution was added to Reservoirs 2 and 1, and then Reservoir 3.

7. Step 6 was repeated once.

2.2.6. Single-cell selection and drug delivery

1. After the chip was washed, as much of the cell medium as possible was removed from only Reservoir 1. Then, the cell suspension in the vial was gently pipetted up and down (see appendix A, note 10). A small cell aliquot of 5 µL was injected into Reservoir 1.

2. After the cell suspension was added to Reservoir 1, a small amount of medium solution was removed to ensure the free movement of cells in the channels.

3. A single cell was selected by placing a small aliquot (1 µL) of medium to push the cell into the V-shaped cell retention structure. The cell was incubated for 5-10 minutes for adhesion f(see appendix A, note 11).

4. The selected glioma cell was loaded with the dye by adding 5 µM of Fluo 4 AM ester. The aperture window was adjusted to enclose the single cell (see appendix 1, note 12). The fluorescence measurement was started. After the introduction of Fluo 4 AM, it took around 600 s for the cell to become fully loaded with the fluorescence calcium probe, as seen in Figure 1.2.

5. The cell was treated with 5 µM and 10 µM of curcumin by applying the test reagent to Reservoir 2 (see appendix A, note 13). The increase in fluorescence intensity indicated elevations in the cellular calcium ion concentration.

6. 10 µM ionomycin (containing 50 µM calcium chloride solution) was introduced to the cell at 2000 s to acquire the highest fluorescence intensity (F_{max}), as shown in Figure 5; this was done to saturate Fluo 4 inside the cell.

7. The fluorescence intensity was converted to intracellular calcium concentration using Equation 1:

$$[Ca^{2+}]_i = K_d \frac{F - F_{min}}{F_{max} - F} \qquad (1)$$

where F shows measured fluorescence; K_d represents dissociation constant of Fluo 4-Ca^{2+} that has the value of 0.35 μM;[14] F_{min} is background fluorescence intensity (in the calcium-free surrounding solution); F_{max} indicates maximum fluorescence induced by ionomycin that facilitates calcium entry through the cell membrane to saturate Fluo 4 .[131]

8. Before compound addition, or when the cell is in the resting condition, F_{min} was obtained from 0 to 500 s when dye loading had begun. F_{max} was obtained at the end of the experiment.

2.2.7. Maintenance of the glass microfluidic chip

During the microfluidic experiment, small particles or cellular debris may cause a channel or reservoir to be clogged, or result in fragment residues that may impact future experiments. Therefore, the following protocol outlines the appropriate steps to efficiently and effectively clean a glass microfluidic chip in order to maintain the integrity of future experimental results.

1. Constant suction was applied to Reservoir 3 of the microfluidic chip.

2. A steady flow of ddH_2O was added through Reservoirs 1 and 2.

3. Step 2 was repeated twice.

4. An aliquot (5 μL) of soap solution was added to Reservoirs 1 and 2, while constant suction was applied to Reservoir 3 to flush the cleaning solution through the microfluidic chip (see appendix A, note 15).

5. Step 4 was repeated four times.

6. Excess soap solution was removed by applying a steady flow of ddH2O through Reservoirs 1 and 2.

7. Step 6 was repeated twice.

8. 5 μL of 70% ethanol was added to Reservoirs 1 and 2, while constant suction was applied to Reservoir 3 to remove the liquid through the microfluidic chip.

9. Step 8 was repeated twice. Then, suction was applied to each reservoir to allow the evaporation of excess ethanol from the channels and/or reservoirs.

10. A 30-minute wait followed until the microfluidic chip was air-dried. The chip was checked under the microscope to ensure that no channels were clogged, and the chamber was clean. The chip was then stored for future experiments.

2.3. Cell calcium bulk analysis

Increase in cytosolic calcium concentration can be measured by bulk analysis of cellular calcium utilizing a 96-well plate and fluorescent microplate reader. This method can be done in several steps illustrated in Figure 2.3.
Details of each step will be elaborated in methodology section.

Figure 2.3. Different steps of cell calcium bulk analysis

2.3.1. Cell line preparation

Desired cell line (cell number and volume required are more than the single cell experiments) was prepared according to the experiment and procedure previously mentioned in this chapter.

2.3.2. Loading cells on a 96-well plate

After adequate confluency of cells, 2 mL of trypsin-EDTA was added based on the cell sub-culturing procedure mentioned above. A 50 µL sample of the cell suspension was taken from the original cell suspension and mixed with 50 µL of trypan blue. The final solution was mixed and prepared for cell counting. The glass cover was located on top of the hemocytometer in its middle as shown in Figure 2.4.

Figure 2.4. A picture of a hemocytometer which was used for cell counting

10µL of cell suspension and trypan blue was added to the top V-groove and 10 µL was added to the bottom V-groove under the glass cover therefore the liquid spreads all under the glass cover.

Then, the hemocytometer was placed under a microscope for counting. Trypan blue can diffuse inside and stain the dead cell's membrane whereas healthy cells can be observed as bright circles under a microscope. The number of bright cells which represent live cells was counted in the four blue squares as shown in Figure 2.5 and the following formula was used to determine the number of cells in the original suspension.

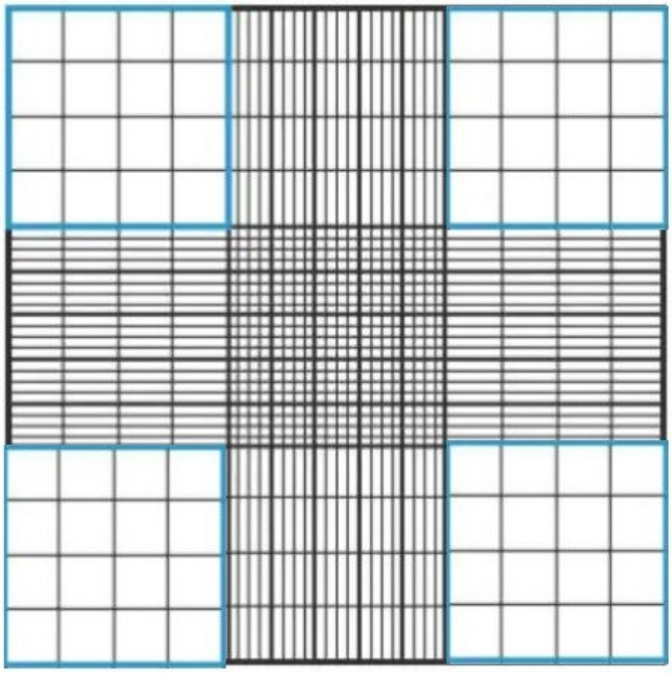

Figure 2.5. Chamber of hemocytometer under microscope

Number of cells in 1 mL of cell suspension

= (Total number of live cells in blue squares/4) * dilution factor*10000,

Where the dilution factor is 2 because of the 1:1 dilution ratio the total number is 400, the number of cells per mL = 400/4 *2 *10000 = 2000000 cells per mL.

After counting, an equal number of 40,000 cells were seeded in each well of the cell culture grade 96 well plate. The black fluorescent microplate with clear bottom must be used. Each well in the 96-well plate had been coated to enable the attachment of cells to the bottom surface. The 96-well plate was incubated overnight and cell attachment was confirmed the next morning under the microscope.

2.3.3. Fluo 4 AM dye loading

After cell attachment, the cell media was removed and cells were washed with HBSS (This washing step is optional) and then 20 µL of 5 µM Fluo 4 AM solution was added in each well with final volume of 180 µL in each well. Next, the cell plate was incubated for 15 minutes at room temperature followed by 15 minutes in the incubator. This incubation was done to have enough time to absorb Fluo 4 AM and convert it to fluorescence active molecule Fluo 4 which can eventually bind to calcium.

After the Fluo 4 AM loading process, 96-well plate was washed with HBSS to remove excess Fluo 4 AM and was prepared for the reagent addition.

Another 96-well plate was needed to prepare the combinations of reagents (reagent plate). A low-cost transparent 96-well plate can be used since this plate is only for reagent use and will not be used for fluorescent studies. All cannabinoid and terpene combinations were prepared in the reagent microplate and were transferred to the cell microplate according to Figure 2.6. Note that in order to make the reagent plate you need to add 50 µL of HBSS inside each well plus the compound (with appropriate volume based on the final concentration) that needs to be tested otherwise the compound (without the addition of HBSS) will be evaporated before transferring that into the cell plate for cell stimulation and calcium measurement.

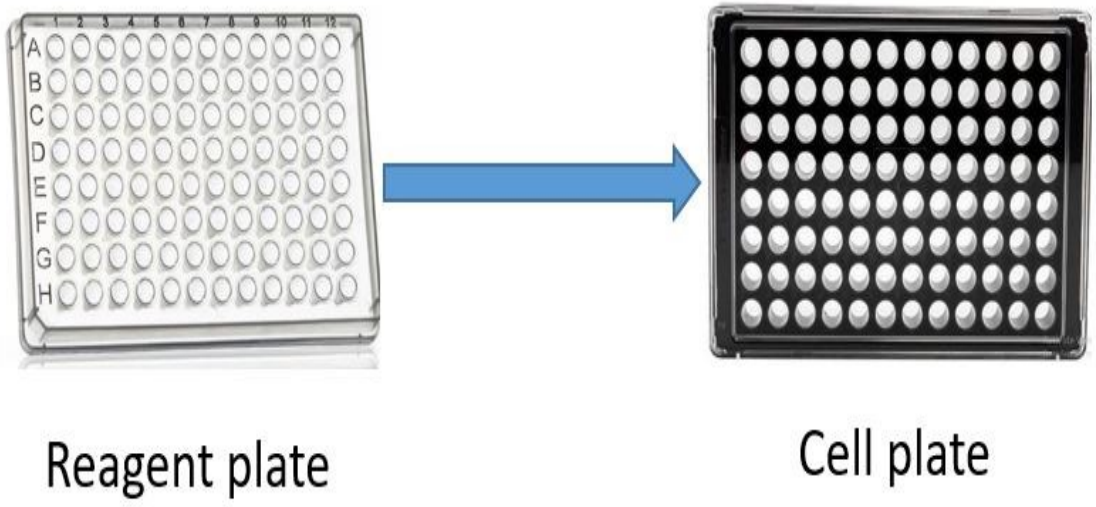

Figure 2.6. Transferring the combinations of cannabinoids and terpenes from the reagent plate to the cell plate

2.3.4. Fluorescence assay on a 96 well plate

The fluorescent intensity of dye-loaded U-87 MG cells was measured in a black clear-bottom COC-coated 96-well plate (Corning NY USA) at a density of 10000 cells per well in HBSS. All the measurements were performed with a Tecan M200 plate reader (Tecan, Switzerland). The following settings were used on the Tecan iControl software for measurements: fluorescence bottom reading (which is a more sensitive mode for working with adherent cells compared to top reading mode), 470 nm excitation wavelength, 530 nm emission wavelength, 25 flashes, 20 μs integration, 0 μs lag time, 0 μs settle time.

In the measurement process, reagents of different combinations were added to the cell plate according to Figure 2.6, and HBSS was added to top up the volume of each well to 180 µL and the measurements was done (F). In the second part of measurements, ionomycin (a calcium ionophore) used to facilitate the transfer of calcium inside the cell to saturate all loaded dye and to increase the fluorescence intensity to F_{max}. The maximum fluorescent value depends on factors such as final number of cells attached in each well. The final concentration of ionomycin in each well was 20 µM. In addition, 180 µL of each reagent-containing HBSS was added to an empty well to represent the background fluorescence intensity or F_{min} of each combination. These measurements were repeated three times. Lastly, by having the F_{max}, F_{min}, and F, the cytosolic calcium concentration due to the treatment of each combination can be calculated by equation 1 (p 43).

2.4. Materials for measurement of changes in cytosolic calcium concentration of A549 cells

2.4.1. Solvents and growth medium

1. DMSO (99.9%)

2. DMEM/High Glucose medium. Supplement this growth medium with sodium pyruvate, 10% fetal bovine serum (FBS), and 1% penicillin.

2.4.2. Cells

1. ACE2-enriched A549 cells were obtained from Invivogene (San Diego, CA) and wild type A549 cells) from American Type Culture Collection.

2. The cells were cultured in the DMEM growth medium in a 5% CO2 atmosphere at 37 °C.

2.4.3. Buffers and enzymes

1. Hanks' Balanced Salt Solution (HBSS).

2. Phosphate-buffered saline (PBS).

3. 0.05% Trypsin-EDTA.

2.4.4. Dyes

1. Fluo 4 AM ester (50 µg, special packaging). Fluo 4 AM ester was dissolved in 50 µL DMSO to prepare a 1 mg/mL stock solution of the fluorescent calcium probe. Since Fluo 4 AM is a light-sensitive dye, it had to be stored in darkness at 20 °C. The stock was freshly diluted before use in HBSS to make a 5.0 µM solution.

2. Trypan blue solution (0.4%). This solution was used to test the viability of the cell under the microscope. Dead cells became stained after the addition of trypan blue.

2.4.5. Test reagents for cell stimulation by histamine

1. Histamine dihydrochloride, 98+%, obtained from Thermo Scientific Chemicals Histamine was dissolved in deionized water to make a stock solution of 100 µM and then diluted in HBSS to produce 5 µM and 10 µM working solutions.

2.4.6. Test reagents for cell stimulation by Ang (1-7)

1. 10 mg of Ang (1-7) obtained from Tocris Bioscience was dissolved in 11.1 µL of deionized water to make a stock solution of 1 M. The stock solution was diluted in HBSS with a dilution ratio of 1:10 to make working solutions.

2.5. Materials for measurement of changes in cytosolic calcium concentration of U-87 MG cells induced by different combination of cannabinoids:

Hank's balanced salt solution (HBSS) and phosphate-buffered saline (PBS) were obtained from Thermofisher (MA, USA). Tetrahydrocannabinol (THC), cannabinol (CBN), cannabichromene (CBC), cannabicyclol (CBL), cannabigerol(CBG), cannabidiol (CBD),

limonene(LME), beta-caryophyllene (BCE) and myrcene (MYR) were purchased from Cedarlane labs (ON, CA).

Fluo 4 AM ester (50 µg, special packaging) was obtained from Molecular Probes (Eugene, OR). It was first dissolved in 50 µL of dimethyl sulfoxide (DMSO, 99.9%, Sigma-Aldrich, St. Louis, MO) to make a stock solution (1 mg mL^{-1}). It was freshly diluted in Hanks' balanced salt solution to make a 5-µM working solution. Ionomycin (IM) and penicillin were also purchased from Sigma-Aldrich. IM was dissolved in DMSO to make a stock solution. Then a 10 mg mL^{-1} ionomycin solution containing 50 mM $CaCl_2$ was prepared as a working solution.

U-87 MG cells (ATCC, USA) were obtained from cryopreserved storage and were maintained in DMEM/High Glucose, pyruvate (ThermoFisher Scientific), containing 10% FBS (ThermoFisher Scientific), and 1% Penicillin (Stemcell Technologies) in a 5% CO_2 atmosphere at 37 °C. The doubling time for the cell the line was approximately 39 h; hence, the growth medium was changed two times a week, and cells were passaged once a week. 0.05% Trypsin-EDTA (ThermoFisher Scientific) was used to detach cells, and 0.4% trypan blue solution (ThermoFisher Scientific) was used to ensure the viability of the cell under the microscope. Dead cells became stained after the addition of trypan blue and alive cells could be observed as bight circles.

Chapter 3. Results and discussion

3.1. Histamine-induced changes of cytosolic calcium concentration in ACE2-overexpressing and wild-type A549 cells

Figure 3.1 illustrates the change in the concentration of cytosolic calcium derived by single-cell analysis of A549 cells. The variations in intensities in the fluorescence measurements have been normalized by the calculation of calcium concentration using equation 1. The cytosolic calcium concentration of the wild type A549 cell is low at rest but it increases after the addition of histamine. The increase of cytosolic calcium in A549 cells is greater when the histamine concentrations increase from 5 μM to 10 μM, and finally to100 μM.

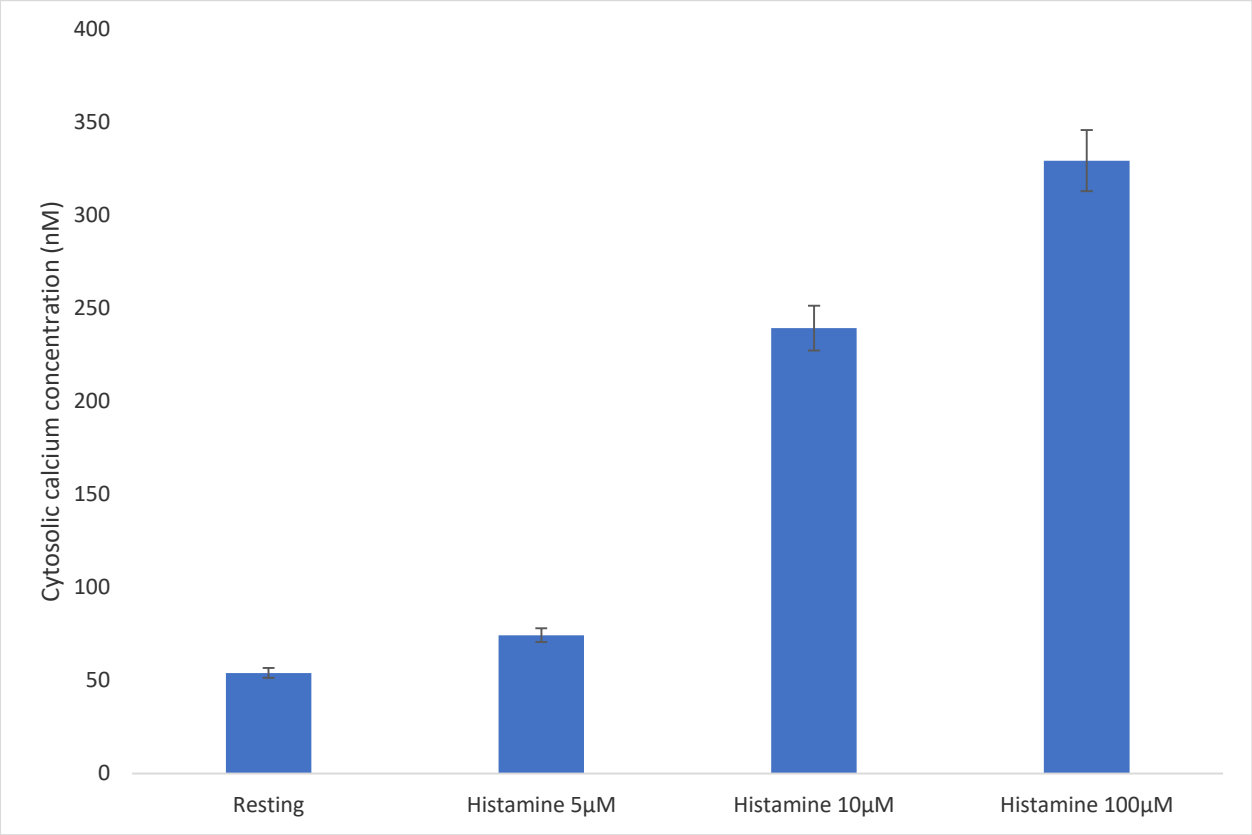

Figure 3.1. Changes of cytosolic calcium in a single A549 cells after the stimulation by different concentrations of histamine. Error bars represent the standard deviation of three measurements (n=3).

The changes of cytosolic calcium due to histamine are also measured in ACE2-enriched A549 cells. Figure 3.2 shows the concentration of cytosolic calcium in single wild-type and ACE2-enriched A549 cells. In terms of statistical difference between resting and 5µM of histamine the t-test value showed $t(4)=8.84$ and p value $p=0.0009$ which shows statistical significance of results. As previously discussed in chapter 1, since A549 cells express both H1 and H2 histamine receptors, [102]the activation of H1 receptors in A549 cells had increased cytosolic calcium concentration. Past research papers also observed an increase in cytosolic calcium concentration in A549 cell using Fura 2 as calcium indictor dye. [106] However, the previous study was not performed at the single-cell scale. Furthermore, the difference between the increases in cytosolic calcium in wild-type A549 and ACE2-overexpressing A549 cells were not studied before.

After adding different concentrations of histamine from 5 μM to 10 μM, and finally to 100 μM, the increase in the cytosolic calcium concentration of wild-type A549 cells is greater than those of ACE2-enriched A549 cells. As compared to ACE2-enriched cells, the wild type A549 has a lower resting level of calcium, but its increase after the addition of histamine is more intense, i.e. for 100 μM histamine, an increase of 6.5-fold (wild type) vs. 2.6-fold (ACE2) was observed which shows potential different expression of histamine receptors in the aforementioned cell lines.

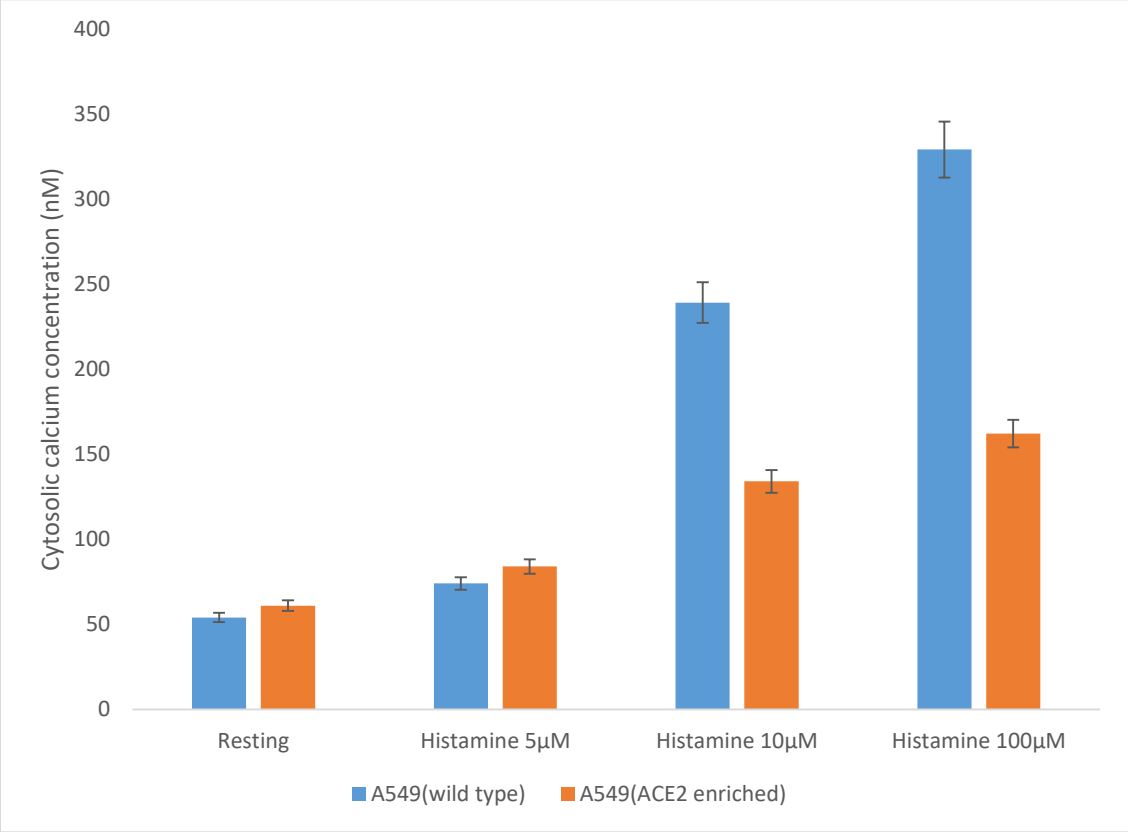

Figure 3.2. Comparison between cytosolic calcium concentration of A549 wild type and A549 ACE2 enriched after the addition of different concentrations of histamine by single-cell analysis (n=3).

Figure 3.3 illustrates the changes in the concentration of cytosolic calcium measured by bulk cell analysis of wild-type and ACE2-enriched A549 cells. The same pattern of cytosolic calcium increases in A549 cells in response to histamine stimulation compared to that of A549

ACE2 enriched cells has been observed. The statistical analysis in resting condition shows t-test value of t(4)=5.56 and p value of p=0.0051. This comparison shows that the difference in the concentration of wild type A549 cells and ACE2 enriched A549 is statistically significant. This observation strengthens the notion that ACE2-enrichment on A549 cells results in smaller response as compared to wild-type A549.

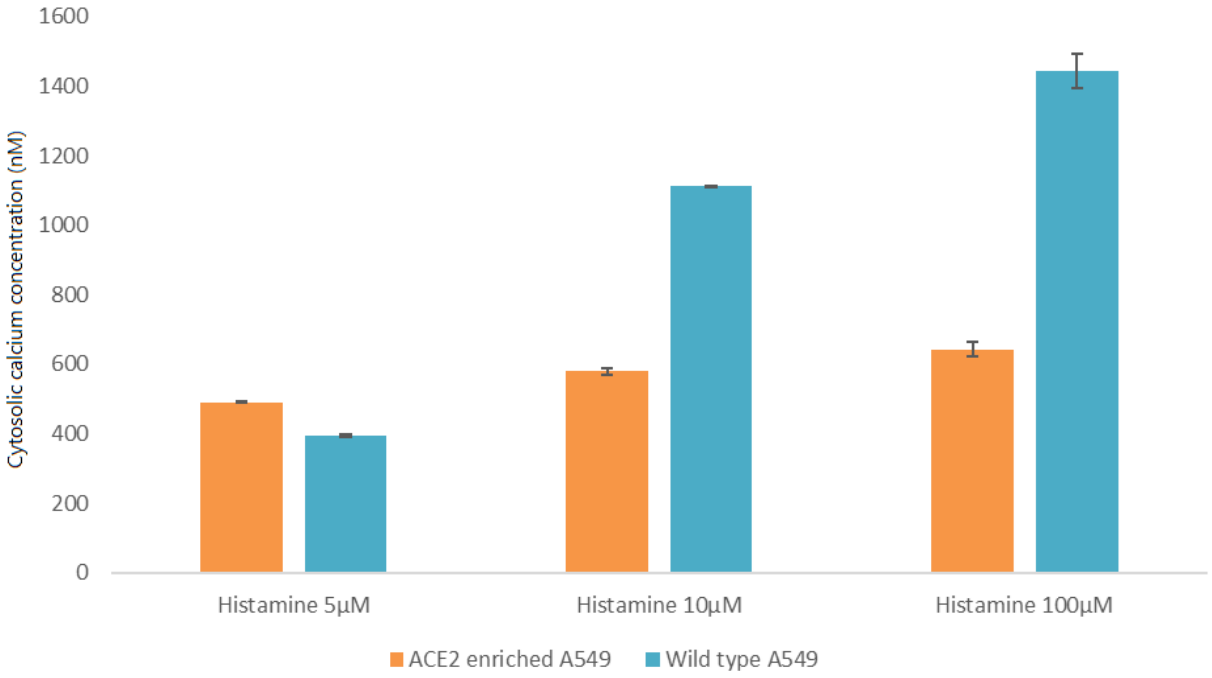

Figure 3.3. Bulk analysis of cytosolic calcium concentration of ACE2 enriched A549 cells and wild type A549 simulated by different concentration of histamine (n=3).

3.2. Ang(1-7) -induced changes in cytosolic calcium concentration of ACE2 overexpressing A549 versus wild-type A549 cells

The single-cell microfluidic experiment was performed with A549 wild-type cells and using different concentrations of Ang (1-7) with concentrations of 0.0001 M, 0.001 M, 0.01 M,

0.1 M and 1 M. One microliter of each concentration of Ang (1-7) was added to the biochip reagent reservoir in all of this section. The purpose of this experiment was to examine different responses in wild type vs. ACE2 overexpressing A549 by Ang(1-7) stimulation. Figure 3.4 illustrates the graph of fluorescent intensity versus time obtained by Felix software which can be transformed to cytosolic calcium concentration by using equation 1, which shows various calcium peaks. These peaks were obtained by measuring the cell fluorescence versus the background by the translation of the chip to move the cell within and outside the measurement window. However, there is no sharply stand-out cytosolic calcium increase observed due to the addition of Ang (1-7). Results show that the cytosolic calcium concentration did not increase and remained at a constant level, see Figure 3.5. These observations may be caused by a number of reasons, e.g. wild-type A549 cells did not possess MAS receptor (see Figure 1.13), or Ang (1-7) did not bind to MAS in these cells, or the binding did not lead to its activation. Therefore, the next experiments were performed on single ACE2-encriched A549 cells. The intensities were calibrated before the experiment using calibration fluorescent beads.

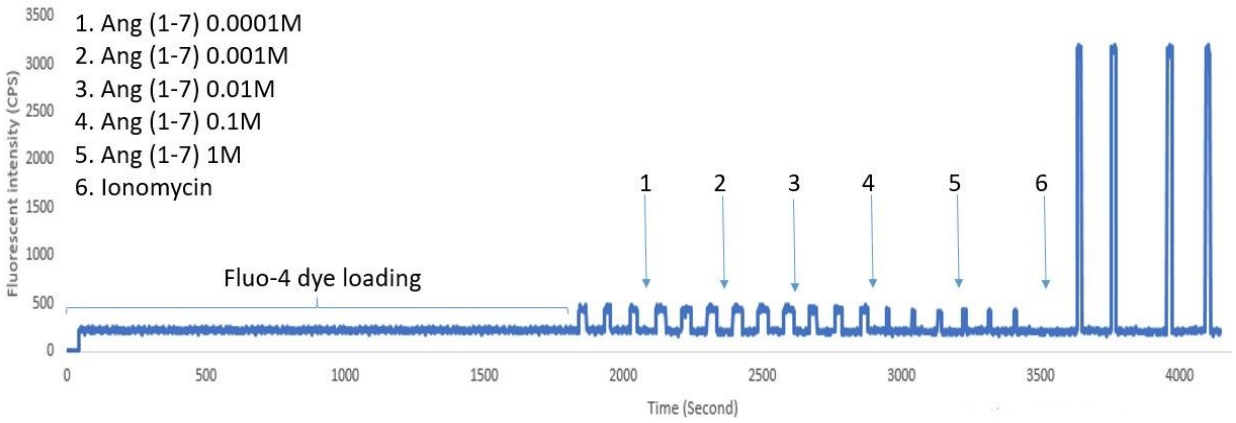

Figure 3.4. Fluorescent intensity versus time obtained from A549 wild type cell stimulated by Ang(1-7) using the Felix software. The four high peaks came from the response to 10 µg/mL ionomycin.

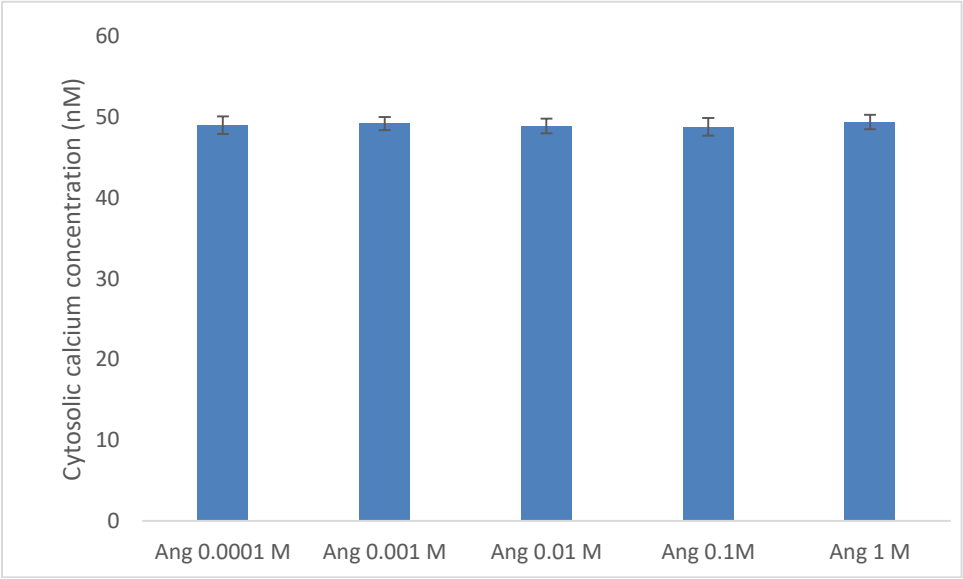

Figure 3.5. Cytosolic calcium concentration obtained from A549 wild type cells simulated by different concentration of Ang(1-7), no change in intracellular calcium concentration was observed

The single-cell microfluidic experiment was performed with ACE2-enriched A549 cells and utilizing same set of concentrations of Ang (1-7) i.e. 0.0001, 0.001, 0.01, 0.1 and 1 M. One microliter of each concentration of Ang (1-7) was added to the biochip reagent reservoir. It was thought that higher expression of ACE2 in the enriched A549 cells might eventually cause an increase in the cytosolic calcium concentration. In contrast, Figure 3.6, which illustrates the graph of fluorescent intensity versus time, showed no change in cytosolic calcium concentration even in ACE2 enriched cells due to Ang (1-7). In these enriched cells, like the wild-type cells, the cytosolic calcium concentration did not increase and remained at a constant level. A comparison between cytosolic calcium concentration in ACE2-enriched cells and wild-type A549 cells is shown in Figure 3.7. In summary, wild-type and ACE2-enriched A549 cells had no effect on the cytosolic calcium concentration. These observations may be caused by a number of reasons, e.g. both types of A549 cells did not possess MAS receptor, or Ang (1-7) didn't bind to MAS in these cells to lead to its activation.

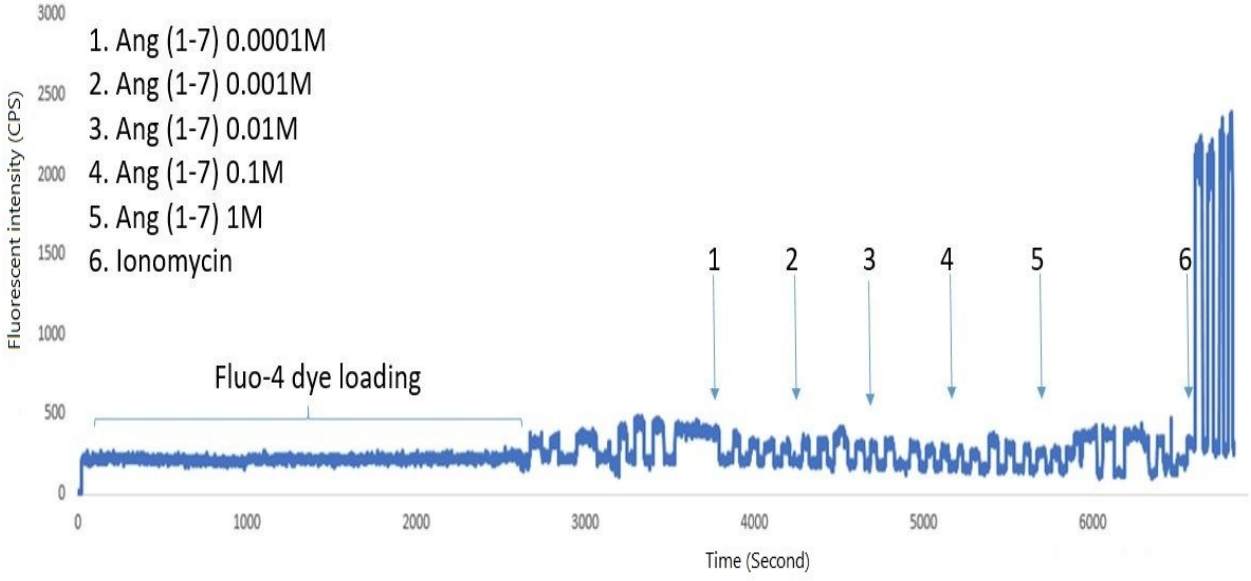

Figure 3.6. Fluorescent intensity versus time obtained from ACE2 enriched A549 cell stimulated by Ang(1-7) using the Felix software.

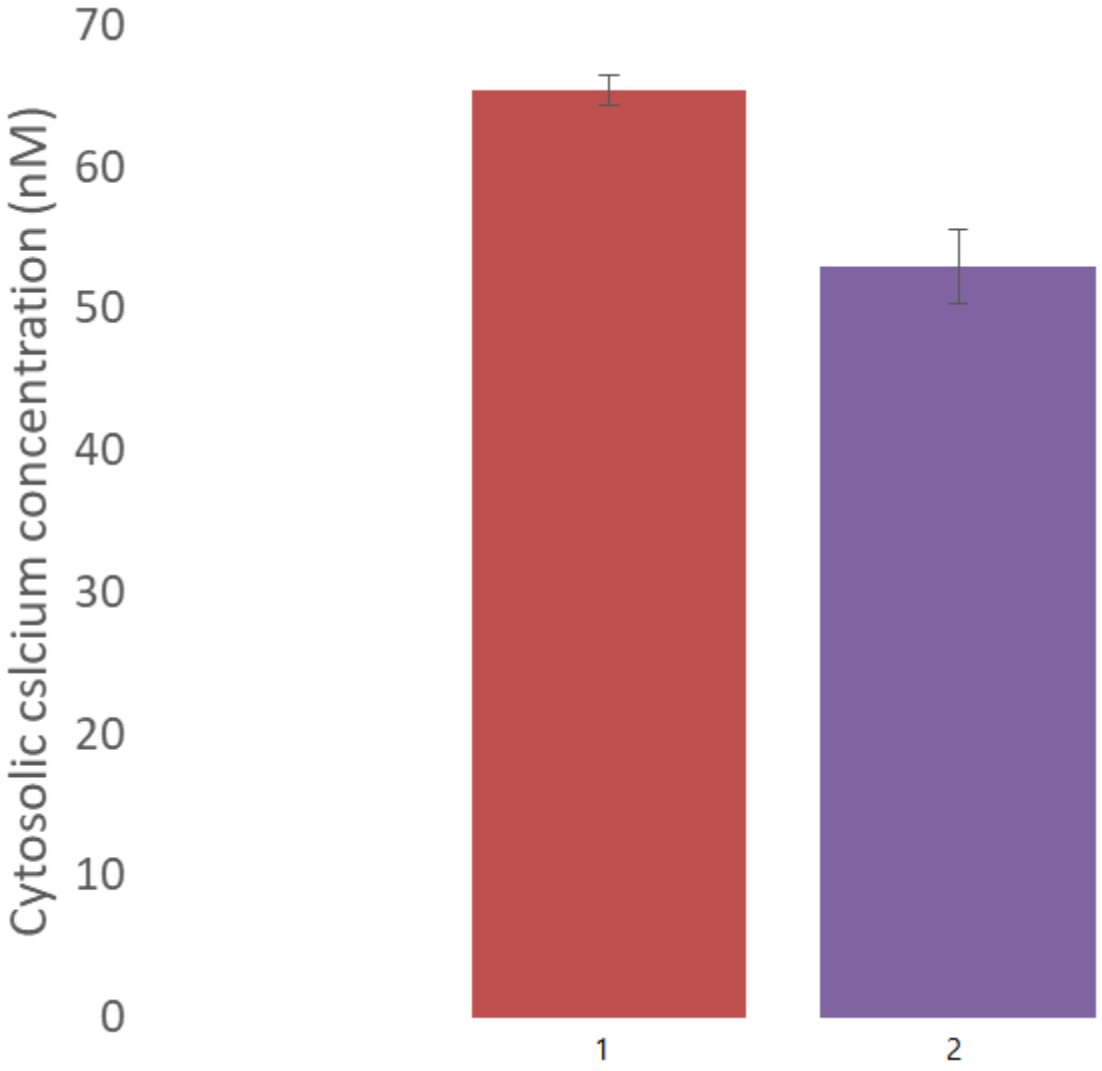

Figure 3.7. A comparison between cytosolic calcium concentration in ACE2-enriched cells and wild-type A549 cells. 1, Resting and Ang(1-7)stimulated A549 ACE2 enriched cell. 2, Resting and Ang(1-7) stimulated A549 wild tye cell (n=3).

.

Ang (1-7) was found to increase cell calcium in U-87 MG cells, which is a glioblastoma cell line. Figure 3.8 illustrates the fluorescent intensity versus time graph of a single U-87 MG cell in response to 0.0001, 0.001, 0.01, 0.1, and 1 M Ang (1-7). The cytosolic calcium concentration peak was observed to be increasing. After the conversion of fluorescent intensities from Figure 3.8 to calcium concentration, its increasing trend is shown in Figure 3.9.

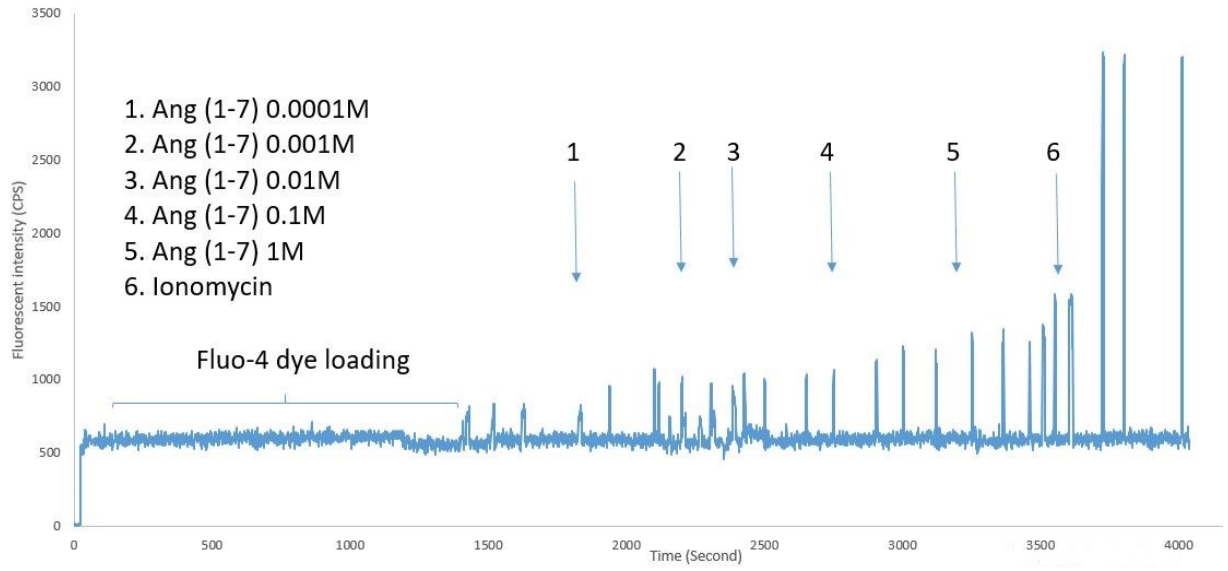

Figure 3.8. Fluorescent intensity versus time obtained by Fleix software using U-87 MG single cell in response to different concentration of Ang(1-7).

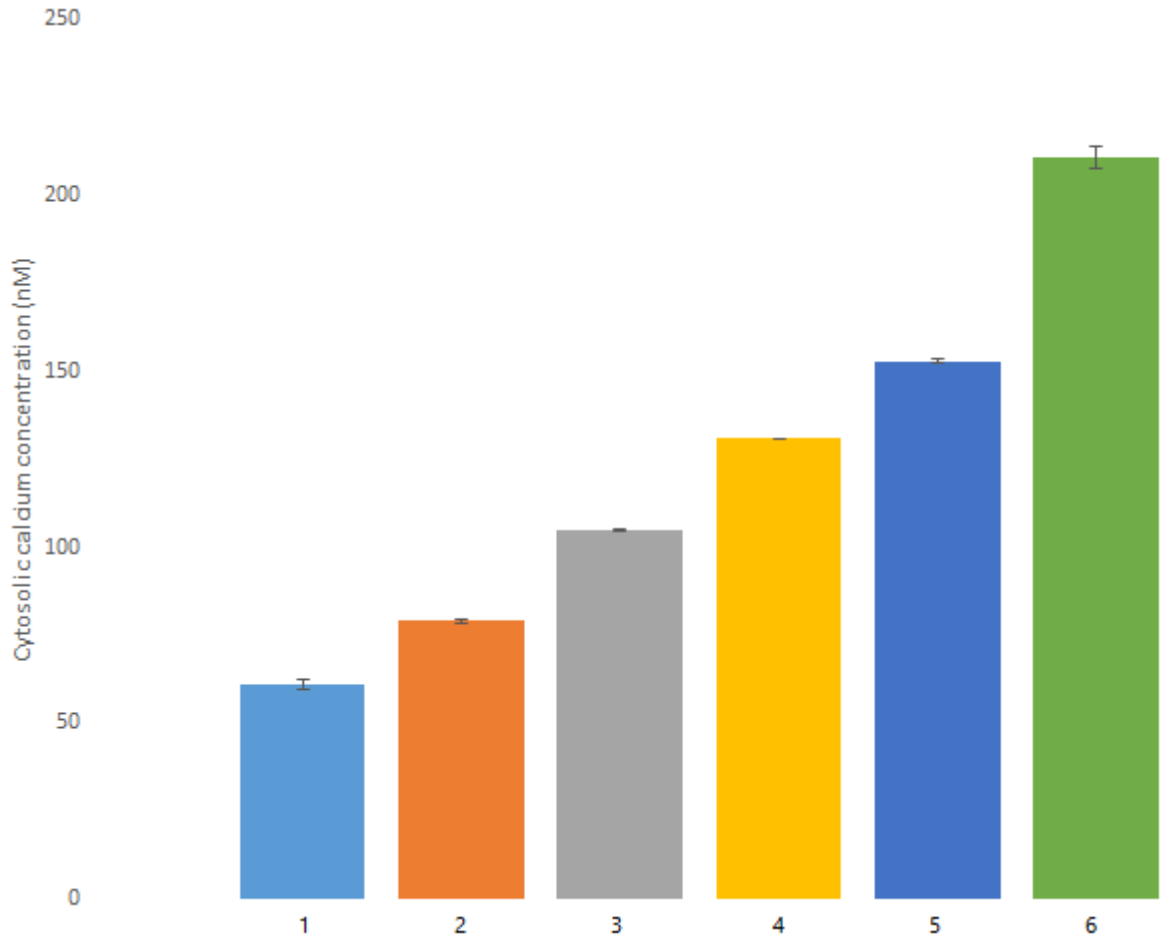

Figure 3.9. Cytosolic calcium concentration change after addition of different concentration of Ang (1-7) in U-87 MG cells. 1, Ang (1-7) 0.0001M. 2, Ang (1-7) 0.001M. 3, Ang (1-7) 0.01M. 4, Ang (1-7) 0.1M. 5, Ang (1-7) 1M. 6, Ionomycin (n=3).

In conclusion, the single-cell microfluidic experiments performed with both wild-type A549 cells and ACE2-enriched A549 cells aimed to investigate the cellular response to different concentrations of Ang (1-7). The results indicated a consistent level of wild-type cells and ACE2-enriched cells which didn't change with varying concentrations of Ang (1-7). These findings suggest that neither wild-type nor ACE2-enriched A549 cells exhibited a noticeable change in cytosolic calcium concentration in response to Ang (1-7) stimulation. Possible explanations include ineffective binding of Ang (1-7) to MAS, or the lack of subsequent activation. Interestingly, U 87 MG glioblastoma cells showed an increase in cytosolic calcium concentration with Ang (1-7) stimulation. However, the specific mechanism for this response in

U-87 MG cells remains unidentified. These findings shed light on the complex and cell specific response to Ang (1-7) and highlights the importance of further exploration into the underlying mechanisms of these observations.

3.3. Cannabinoids induced changes in cytosolic calcium concentration of U-87 MG cells

Scientists study intracellular calcium as a fundamental tool to probe and understand the diverse responses triggered by different combinations of cannabinoids.[132] These compounds, derived from the cannabis plant, interact with specific receptors in the endocannabinoid system, leading to an increase in intracellular calcium levels. These increase are caused by activation of different GPCRs such as cannabinoid receptor type 1, cannabinoid receptor type 2, transient receptor potential vanilloid 1 (TRPV1). [133] By measuring these fluctuations, researchers gain insights into cannabinoids influence in cellular processes, such as immune response, neurotransmission, and apoptosis. In this research sixty different combinations of cannabinoids were investigated, to measure the changes in bulk cytosolic calcium concentration of U-87 MG cells. The final data, determined from equation 1, represents the cytosolic calcium concentration (in nM). Standard deviations were also determined from three measurements in bulk cells using a 96-well plate. The complete results of 60 different combinations of cannabinoids are illustrated in Figure 3.10.

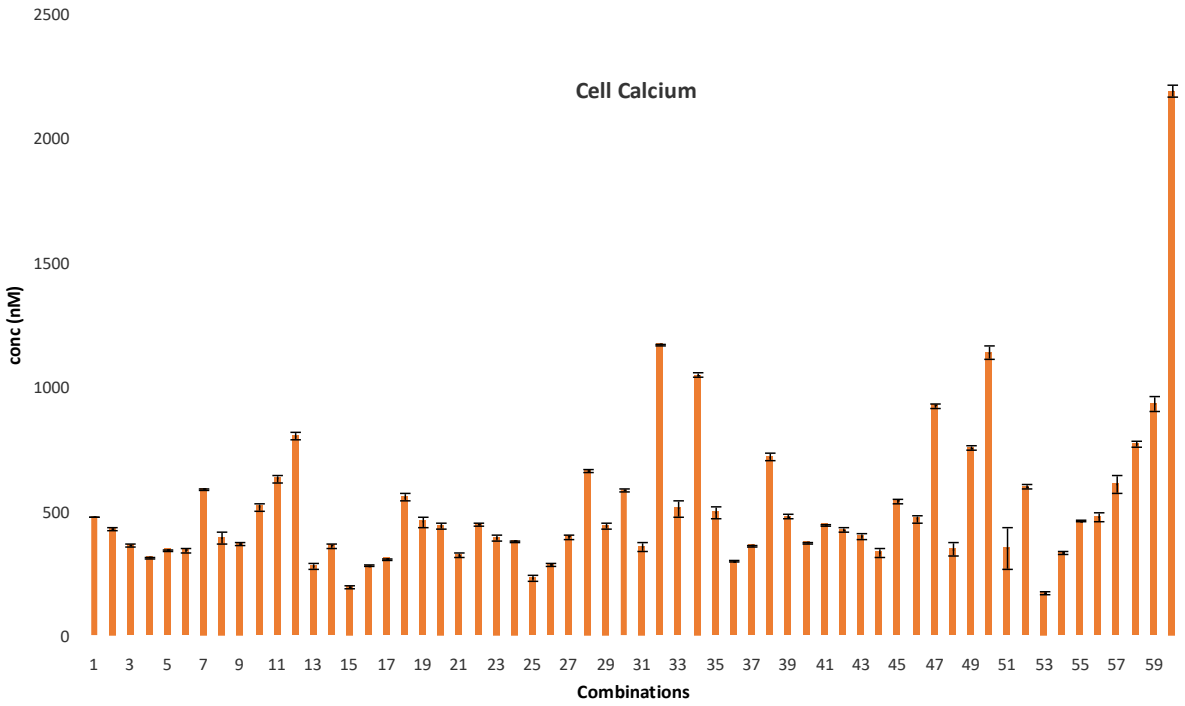

Figure 3.10. Cytosolic calcium concentration of U-87 MG cells after addition of 60 different combinations of cannabinoids (n=3).

In conclusion, the combinations involve compounds such as Tetrahydrocannabinol (THC), cannabinol (CBN), cannabichromene (CBC), cannabicyclol (CBL), cannabigerol(CBG), cannabidiol (CBD), limonene(LME), beta-caryophyllene (BCE) and myrcene (MYR). It is found the combinations 32, 34, 50 and 60 gave the highest cell calcium response. Further testing on single cells will be performed to verify the findings. Moreover, AutoDock Vina, which is a molecular modeling simulation software, would be used to simulate the responses of various cannabinoid combinations that would affect the receptors such as TRPV1, TRPC5, which are overexpressed in U-87 MG cells.

Chapter 4. Conclusion and future work

4.1. Single-Cell vs. Bulk-Cell Calcium Measurement

The single-cell approach measures a single cell's calcium response. This method provides high temporal resolution and enables the observation of intricate, cell-specific details of calcium signaling. However, the method lacks the sample throughput and the ability to detect the broad context of cell heterogeneity present in a population. On the contrary, the bulk-cell calcium measurement approach offers a global view of cellular responses by analyzing a population of cells simultaneously. This approach provides the necessary throughput and allows researchers to understand the collective behavior of cells on calcium signaling.

4.2. Integration of Single-Cell and Bulk-Cell Approaches

Combining single-cell and bulk-cell analyses offers a comprehensive understanding of cellular calcium homeostasis. The single-cell approach identifies specific cellular behaviours, whereas the bulk-cell analysis provides an overall picture of responses within a population of cells. This integration may unravel correlations between individual cell responses and population-wide trends.

4.3. Experimental Findings

In the context of the research presented, the effects of histamine on $[Ca^{2+}]_i$ were investigated utilizing both single-cell and bulk-cell calcium measurement methods. Histamine was found to elevate cytosolic calcium concentration in both cell types of A549, though the elevation was greater in the case of wild-type cells versus ACE2-enriched cells. However, results conclude that although Ang (1-7) caused an increase in $[Ca^{2+}]_i$ U-87 MG cells, but the endogenous molecule did not lead to such an increase in wild-type and ACE2-enriched A549 cells.

4.4. Development of Bulk-Cell Calcium Measurement Method

The study introduced a bulk-cell measurement method based on cytosolic calcium assays using a 96-well plate format. This method offers a high-throughput approach for analyzing intracellular calcium levels in a large number of cells simultaneously. Combinations of

cannabinoids (CBD, CBN, CBC, CBL, CBG) and terpenes (BCE, LME and MYR) were tested, resulting in a substantial increase in cell calcium concentration provided by several combinations. The potency of these compounds underscores their potential relevance in some pain receptor pathways.

4.5. Future Directions

The research outlines promising avenues for further exploration. To delve deeper into cellular calcium dynamics, investigations of the calcium content in subcellular organelles using high-magnification optics and sensitive detection methods will be required. Additionally, incorporating multiple trapping sites and cell retention structures on a chip could enhance the efficiency and throughput of single-cell calcium measurement experiments, enabling precise cellular analysis.

4.6. Implications for COVID-19 Research

The thesis may suggest potential applications of cytosolic calcium in the context of COVID-19 research. By using antagonists, MAS receptor blockers, and the spike protein of SARS-CoV-2, researchers may observe cell calcium changes due to the potential blockage of the MAS receptor and disruption of the renin-angiotensin system. Changes in cytosolic calcium concentration induced by these blockers may serve as indicators of successful SARS-CoV-2 viral entry inhibition. This novel avenue could contribute to the development of therapeutic interventions for COVID-19 treatment.

4.7. Summary

In conclusion, our research has shed light on the intricate landscape of calcium signaling dynamics at both the single-cell and bulk-cell levels. The research findings demonstrate the significance of these methods in understanding cellular responses to various stimuli, including histamine and Ang(1-7) study in wild-type and ACE2-overexpressing A549 cells, or cannabinoid study in U-87 MG cells. Furthermore, the development of a bulk-cell calcium measurement method highlights the potential of cannabinoids and terpenes in modulating cellular calcium dynamics in some receptor models. Notably, our research may contribute to the field of COVID-19 research by investigating the wild-type and ACE2-overexpressing A549 cells, perhaps after the expression of the MAS receptor, in the context of changes in cytosolic calcium

concentration.

References

1. Wheeler, A. R. *et al.* Microfluidic device for single-cell analysis. *Anal Chem* **75**, 3581–3586 (2003).
2. Francesko, A., Cardoso, V. F. & Lanceros-Méndez, S. Chapter 1 - Lab-on-a-chip technology and microfluidics. in *Microfluidics for Pharmaceutical Applications* (eds. Santos, H. A., Liu, D. & Zhang, H.) 3–36 (William Andrew Publishing, 2019). doi:10.1016/B978-0-12-812659-2.00001-6.
3. Valls, P. O. & Esposito, A. Signalling dynamics, cell decisions, and homeostatic control in health and disease. *Curr Opin Cell Biol* **75**, None (2022).
4. Gao, J., Yin, X.-F. & Fang, Z.-L. Integration of single cell injection, cell lysis, separation and detection of intracellular constituents on a microfluidic chip. *Lab on a Chip* **4**, 47–52 (2004).
5. Fletcher, K. A. *et al.* Molecular Fluorescence, Phosphorescence, and Chemiluminescence Spectrometry. *Anal Chem* **78**, 4047–4068 (2006).
6. Hogan, B. L. & Yeung, E. S. Determination of intracellular species at the level of a single erythrocyte via capillary electrophoresis with direct and indirect fluorescence detection. *Anal. Chem.* **64**, 2841–2845 (1992).
7. Li, X. & Li, P. C. H. Microfluidic selection and retention of a single cardiac myocyte, on-chip dye loading, cell contraction by chemical stimulation, and quantitative fluorescent analysis of intracellular calcium. *Anal Chem* **77**, 4315–4322 (2005).
8. Li, X., Huang, J., Tibbits, G. F. & Li, P. C. H. Real-time monitoring of intracellular calcium dynamic mobilization of a single cardiomyocyte in a microfluidic chip pertaining to drug discovery. *ELECTROPHORESIS* **28**, 4723–4733 (2007).
9. Paredes, R. M., Etzler, J. C., Watts, L. T., Zheng, W. & Lechleiter, J. D. Chemical calcium indicators. *Methods* **46**, 143–151 (2008).

10. Lee, Y. K., Segars, K. L. & Trinkaus-Randall, V. Multiple Imaging Modalities for Cell-Cell Communication via Calcium Mobilizations in Corneal Epithelial Cells. *Methods Mol Biol* **2346**, 11–20 (2021).
11. Landero-Figueroa, J. A., Vignesh, K. S., Deepe, G. & Caruso, J. SELECTIVITY AND SPECIFICITY OF SMALL MOLECULE FLUORESCENT DYES/PROBES USED FOR THE DETECTION OF Zn2+ AND Ca2+ IN CELLS. *Metallomics* **6**, 301–315 (2014).
12. Dustin, L. B. Ratiometric analysis of calcium mobilization. *Clinical and Applied Immunology Reviews* **1**, 5–15 (2000).
13. Ribeiro, D. *et al.* Calcium Pathways in Human Neutrophils—The Extended Effects of Thapsigargin and ML-9. *Cells* **7**, 204 (2018).
14. Gee, K. R. *et al.* Chemical and physiological characterization of fluo-4 Ca2+-indicator dyes. *Cell Calcium* **27**, 97–106 (2000).
15. Di Carlo, D, L., L. Dynamic Single-Cell Analysis for Quantitative Biology. *Anal. Chem.* **78**, 7918–7925 (2006).
16. He, J.-L., Chen, A.-T., Lee, J. & Fan, S.-K. Digital Microfluidics for Manipulation and Analysis of a Single Cell. *International Journal of Molecular Sciences* **16**, 22319 (2015).
17. Perlman, Z. E. *et al.* Multidimensional drug profiling by automated microscopy. *Science* **306**, 1194–1198 (2004).
18. Eggert, U. S. & Mitchison, T. J. Small molecule screening by imaging. *Current Opinion in Chemical Biology* **10**, 232–237 (2006).
19. Yi, J. *et al.* Development of an electrochemical immunoassay for detection of gatifloxacin in swine urine. *J. Zhejiang Univ. Sci. B* **13**, 118–125 (2012).
20. Kennedy, R. T., Oates, M. D., Cooper, B. R., Nickerson, B. & Jorgenson, J. W. Microcolumn separations and the analysis of single cells. *Science* **246**, 57–63 (1989).
21. Harrison, D. J. *et al.* Micromachining a miniaturized capillary electrophoresis-based chemical analysis system on a chip. *Science* **261**, 895–897 (1993).

22. Auroux, P.-A., Iossifidis, D., Reyes, D. R. & Manz, A. Micro total analysis systems. 2. Analytical standard operations and applications. *Anal Chem* **74**, 2637–2652 (2002).
23. Terry, S. C., Jerman, J. H. & Angell, J. B. A gas chromatographic air analyzer fabricated on a silicon wafer. *IEEE Trans. Electron Devices* **26**, 1880–1886 (1979).
24. Manz, A. *et al.* μ-TAS: Miniaturized Total Chemical Analysis Systems. in *Micro Total Analysis Systems* (eds. Van den Berg, A. & Bergveld, P.) 5–27 (Springer Netherlands, 1995). doi:10.1007/978-94-011-0161-5_2.
25. Karube, I. μTAS for Biochemical Analysis. in *Micro Total Analysis Systems* (eds. Van den Berg, A. & Bergveld, P.) 37–46 (Springer Netherlands, 1995). doi:10.1007/978-94-011-0161-5_4.
26. Kopf-Sill, A. R. Commercializing Lab-on-a-Chip Technology. in *Micro Total Analysis Systems 2000* (eds. van den Berg, A., Olthuis, W. & Bergveld, P.) 233–238 (Springer Netherlands, 2000). doi:10.1007/978-94-017-2264-3_54.
27. Dittrich, P. S., Tachikawa, K. & Manz, A. Micro Total Analysis Systems. Latest Advancements and Trends. *Anal. Chem.* **78**, 3887–3908 (2006).
28. Microfluidic Systems for Diagnostic Applications: A Review - Kin Fong Lei, 2012. https://journals.sagepub.com/doi/full/10.1177/2211068212454853.
29. Wong-Hawkes, S. Y. F., Matteo, J. C., Warrington, B. H. & White, J. D. Microreactors as new tools for drug discovery and development. *Ernst Schering Found Symp Proc* 39–55 (2006) doi:10.1007/2789_2007_027.
30. Lu, S., Giamis, A. M. & Pike, V. W. Synthesis of [18F]fallypride in a micro-reactor. *Curr Radiopharm* **2**, nihpa81093 (2009).
31. Saliterman, S. *Fundamentals of BioMEMS and Medical Microdevices*. (SPIE Press, 2006).
32. Zhan, W., Alvarez, J. & Crooks, R. M. A two-channel microfluidic sensor that uses anodic electrogenerated chemiluminescence as a photonic reporter of cathodic redox reactions. *Anal Chem* **75**, 313–318 (2003).

33. Koutny, L. *et al.* Eight Hundred-Base Sequencing in a Microfabricated Electrophoretic Device. *Anal. Chem.* **72**, 3388–3391 (2000).
34. Simpson, P. C. *et al.* High-throughput genetic analysis using microfabricated 96-sample capillary array electrophoresis microplates. *Proceedings of the National Academy of Sciences* **95**, 2256–2261 (1998).
35. Badal, M. Y., Wong, M., Chiem, N., Salimi-Moosavi, H. & Harrison, D. J. Protein separation and surfactant control of electroosmotic flow in poly(dimethylsiloxane)-coated capillaries and microchips. *J Chromatogr A* **947**, 277–286 (2002).
36. Chen, C. & Folch, A. A high-performance elastomeric patch clamp chip. *Lab Chip* **6**, 1338–1345 (2006).
37. Leng, Y. *et al.* Advances in In Vitro Models of Neuromuscular Junction: Focusing on Organ-on-a-Chip, Organoids, and Biohybrid Robotics. *Advanced Materials* **35**, 2211059 (2023).
38. Gu, W., Zhu, X., Futai, N., Cho, B. S. & Takayama, S. Computerized microfluidic cell culture using elastomeric channels and Braille displays. *Proc Natl Acad Sci U S A* **101**, 15861–15866 (2004).
39. Forry, S. P., Reyes, D. R., Gaitan, M. & Locascio, L. E. Cellular Immobilization within Microfluidic Microenvironments: Dielectrophoresis with Polyelectrolyte Multilayers. *J. Am. Chem. Soc.* **128**, 13678–13679 (2006).
40. Li, P. C. & Harrison, D. J. Transport, manipulation, and reaction of biological cells on-chip using electrokinetic effects. *Anal Chem* **69**, 1564–1568 (1997).
41. Shelby, J. P., White, J., Ganesan, K., Rathod, P. K. & Chiu, D. T. A microfluidic model for single-cell capillary obstruction by Plasmodium falciparum-infected erythrocytes. *Proc Natl Acad Sci U S A* **100**, 14618–14622 (2003).
42. Khine, M., Lau, A., Ionescu-Zanetti, C., Seo, J. & Lee, L. P. A single cell electroporation chip. *Lab Chip* **5**, 38–43 (2005).

43. Lin, Y.-C., Li, M. & Wu, C.-C. Simulation and experimental demonstration of the electric field assisted electroporation microchip for in vitro gene delivery enhancement. *Lab Chip* **4**, 104–108 (2004).
44. Strömberg, A. *et al.* Microfluidic device for combinatorial fusion of liposomes and cells. *Anal Chem* **73**, 126–130 (2001).
45. Packard, M. M., Wheeler, E. K., Alocilja, E. C. & Shusteff, M. Performance Evaluation of Fast Microfluidic Thermal Lysis of Bacteria for Diagnostic Sample Preparation †. *Diagnostics (Basel)* **3**, 105–116 (2013).
46. Klauke, N., Smith, G. L. & Cooper, J. Extracellular Recordings of Field Potentials from Single Cardiomyocytes. *Biophys J* **91**, 2543–2551 (2006).
47. Shields, C. W., Reyes, C. D. & López, G. P. Microfluidic Cell Sorting: A Review of the Advances in the Separation of Cells from Debulking to Rare Cell Isolation. *Lab Chip* **15**, 1230–1249 (2015).
48. McClain, M. A. *et al.* Microfluidic devices for the high-throughput chemical analysis of cells. *Anal Chem* **75**, 5646–5655 (2003).
49. Voldman, J. Engineered systems for the physical manipulation of single cells. *Current Opinion in Biotechnology* **17**, 532–537 (2006).
50. Chung, T. D. & Kim, H. C. Recent advances in miniaturized microfluidic flow cytometry for clinical use. *ELECTROPHORESIS* **28**, 4511–4520 (2007).
51. Cabrera, C. R. & Yager, P. Continuous concentration of bacteria in a microfluidic flow cell using electrokinetic techniques. *Electrophoresis* **22**, 355–362 (2001).
52. Yoshida, M., Tohda, K. & Gratzl, M. Hydrodynamic micromanipulation of individual cells onto patterned attachment sites on biomicroelectromechanical system chips. *Anal Chem* **75**, 4686–4690 (2003).
53. Wilding, P. *et al.* Integrated cell isolation and polymerase chain reaction analysis using silicon microfilter chambers. *Anal Biochem* **257**, 95–100 (1998).

54. Yang, M., Li, C.-W. & Yang, J. Cell Docking and On-Chip Monitoring of Cellular Reactions with a Controlled Concentration Gradient on a Microfluidic Device. *Anal. Chem.* **74**, 3991–4001 (2002).
55. Zhou, J. The Development of the Heparin Monitoring System Based on Microfluidics Technology. *JBNB* **11**, 195–213 (2020).
56. Demaurex, N. Calcium measurements in organelles with Ca2+-sensitive fluorescent proteins. *Cell Calcium* **38**, 213–222 (2005).
57. Mertes, N. *et al.* Fluorescent and Bioluminescent Calcium Indicators with Tuneable Colors and Affinities. *J. Am. Chem. Soc.* **144**, 6928–6935 (2022).
58. Vetter, I. Development and Optimization of FLIPR High Throughput Calcium Assays for Ion Channels and GPCRs. in *Calcium Signaling* (ed. Islam, Md. S.) 45–82 (Springer Netherlands, 2012). doi:10.1007/978-94-007-2888-2_3.
59. Chang, T. C. *et al.* Microwell arrays reveal cellular heterogeneity during the clonal expansion of transformed human cells. *Technology* **03**, 163–171 (2015).
60. Zhang, J., Campbell, R., Ting, A. & Tsien, R. Creating New Fluorescent Probes for Cell Biology. *Nature reviews. Molecular cell biology* **3**, 906–18 (2003).
61. Wigglesworth, M. J. *et al.* Use of Cryopreserved Cells for Enabling Greater Flexibility in Compound Profiling. *J Biomol Screen* **13**, 354–362 (2008).
62. Emkey, R. & Rankl, N. B. Screening G Protein-Coupled Receptors: Measurement of Intracellular Calcium Using the Fluorometric Imaging Plate Reader. *High Throughput Screening* **565**, 145–158 (2009).
63. Gopalakrishnan, S. M. *et al.* An Offline-Addition Format for Identifying GPCR Modulators by Screening 384-Well Mixed Compounds in the FLIPR. *Journal of biomolecular screening* **10**, 46–55 (2005).
64. Miret, J. J. *et al.* Multiplexed G-Protein–Coupled Receptor Ca2+ Flux Assays for High-Throughput Screening. *Journal of biomolecular screening* **10**, 780–787 (2005).

65. Takahashi, A., Camacho, P., Lechleiter, J. D. & Herman, B. Measurement of Intracellular Calcium. *Physiological Reviews* **79**, 1089–1125 (1999).

66. Hauser, A. S., Attwood, M. M., Rask-Andersen, M., Schiöth, H. B. & Gloriam, D. E. Trends in GPCR drug discovery: new agents, targets and indications. *Nat Rev Drug Discov* **16**, 829–842 (2017).

67. Ashley, C. C. & Ridgway, E. B. On the relationships between membrane potential, calcium transient and tension in single barnacle muscle fibres. *J Physiol* **209**, 105–130 (1970).

68. Tsien, R. Y. & Rink, T. J. Neutral carrier ion-selective microelectrodes for measurement of intracellular free calcium. *Biochimica et Biophysica Acta (BBA) - Biomembranes* **599**, 623–638 (1980).

69. Berridge, M. J., Bootman, M. D. & Roderick, H. L. Calcium signalling: dynamics, homeostasis and remodelling. *Nat Rev Mol Cell Biol* **4**, 517–529 (2003).

70. Orrenius, S., Zhivotovsky, B. & Nicotera, P. Regulation of cell death: the calcium–apoptosis link. *Nat Rev Mol Cell Biol* **4**, 552–565 (2003).

71. Rizzuto, R., Brini, M., Murgia, M. & Pozzan, T. Microdomains with high Ca2+ close to IP3-sensitive channels that are sensed by neighboring mitochondria. *Science* **262**, 744–747 (1993).

72. Duchen, M. R. Mitochondria and calcium: from cell signalling to cell death. *J Physiol* **529**, 57–68 (2000).

73. Chen, B.-F., Tsai, M.-C. & Jow, G.-M. Induction of calcium influx from extracellular fluid by beauvericin in human leukemia cells. *Biochem Biophys Res Commun* **340**, 134–139 (2006).

74. Sriram, K. & Insel, P. A. G Protein-Coupled Receptors as Targets for Approved Drugs: How Many Targets and How Many Drugs? *Mol Pharmacol* **93**, 251–258 (2018).

75. Hauser, A. S. *et al.* Pharmacogenomics of GPCR Drug Targets. *Cell* **172**, 41-54.e19 (2018).

76. Katritch, V., Cherezov, V. & Stevens, R. C. Structure-Function of the G-protein-Coupled Receptor Superfamily. *Annu Rev Pharmacol Toxicol* **53**, 531–556 (2013).

77. Dhyani, V. *et al.* GPCR mediated control of calcium dynamics: A systems perspective. *Cell Signal* **74**, 109717 (2020).
78. Qiu, S. *et al.* Small molecule metabolites: discovery of biomarkers and therapeutic targets. *Sig Transduct Target Ther* **8**, 1–37 (2023).
79. Lamichhane, S., Sen, P., Dickens, A. M., Hyötyläinen, T. & Orešič, M. Chapter Fourteen - An Overview of Metabolomics Data Analysis: Current Tools and Future Perspectives. in *Comprehensive Analytical Chemistry* (eds. Jaumot, J., Bedia, C. & Tauler, R.) vol. 82 387–413 (Elsevier, 2018).
80. Puzianowska-Kuznicka, M., Pawlik-Pachucka, E., Owczarz, M., Budzińska, M. & Polosak, J. Small-Molecule Hormones: Molecular Mechanisms of Action. *International Journal of Endocrinology* **2013**, 1–21 (2013).
81. Hedges, V. Introduction to Small Molecule Neurotransmitters. (2022).
82. Hou, S., Heinemann, S. H. & Hoshi, T. Modulation of BKCa channel gating by endogenous signaling molecules. *Physiology (Bethesda)* **24**, 26–35 (2009).
83. Cheong, S., Clomburg, J. M. & Gonzalez, R. Energy- and carbon-efficient synthesis of functionalized small molecules in bacteria using non-decarboxylative Claisen condensation reactions. *Nat Biotechnol* **34**, 556–561 (2016).
84. Ma, Y., Liu, X. & Wang, J. Small molecules in the big picture of gut microbiome-host cross-talk. *eBioMedicine* **81**, (2022).
85. Carlson, E. E. Natural Products as Chemical Probes. *ACS Chem Biol* **5**, 639–653 (2010).
86. Li, Q. & Kang, C. Mechanisms of Action for Small Molecules Revealed by Structural Biology in Drug Discovery. *Int J Mol Sci* **21**, 5262 (2020).
87. Hopkins, M. *et al.* The Control of Food Intake in Humans. in *Endotext* (eds. Feingold, K. R. et al.) (MDText.com, Inc., 2000).
88. Dijkhoff, I. M. *et al.* Impact of airborne particulate matter on skin: a systematic review from epidemiology to in vitro studies. *Part Fibre Toxicol* **17**, 35 (2020).

89. Gonsioroski, A., Mourikes, V. E. & Flaws, J. A. Endocrine Disruptors in Water and Their Effects on the Reproductive System. *International journal of molecular sciences* **21**, (2020).
90. Gurevich, E. V. & Gurevich, V. V. Therapeutic Potential of Small Molecules and Engineered Proteins. *Handb Exp Pharmacol* **219**, 1–12 (2014).
91. Govardhanagiri, S., Bethi, S. & Nagaraju, G. P. Chapter 8 - Small Molecules and Pancreatic Cancer Trials and Troubles. in *Breaking Tolerance to Pancreatic Cancer Unresponsiveness to Chemotherapy* (ed. Nagaraju, G. P.) vol. 5 117–131 (Academic Press, 2019).
92. Houle, M.-C., Holness, D. L. & DeKoven, J. Occupational Contact Dermatitis: An Individualized Approach to the Worker with Dermatitis. *Curr Dermatol Rep* **10**, 182–191 (2021).
93. Li, A. J., Pal, V. K. & Kannan, K. A review of environmental occurrence, toxicity, biotransformation and biomonitoring of volatile organic compounds. *Environmental Chemistry and Ecotoxicology* **3**, 91–116 (2021).
94. Andre, C. M., Hausman, J.-F. & Guerriero, G. Cannabis sativa: The Plant of the Thousand and One Molecules. *Front Plant Sci* **7**, 19 (2016).
95. Holgate, S. T. The epithelium takes centre stage in asthma and atopic dermatitis. *Trends Immunol* **28**, 248–251 (2007).
96. Liu, T., Zhang, L., Joo, D. & Sun, S.-C. NF-κB signaling in inflammation. *Signal Transduct Target Ther* **2**, 17023- (2017).
97. Smolinska, S., Jutel, M., Crameri, R. & O'Mahony, L. Histamine and gut mucosal immune regulation. *Allergy* **69**, 273–281 (2014).
98. Jutel, M., Blaser, K. & Akdis, C. A. Histamine in allergic inflammation and immune modulation. *Int Arch Allergy Immunol* **137**, 82–92 (2005).
99. Thakkar, M. M. Histamine in the regulation of wakefulness. *Sleep Med Rev* **15**, 65–74 (2011).

100. Chang, C.-W. *et al.* A Newly Engineered A549 Cell Line Expressing ACE2 and TMPRSS2 Is Highly Permissive to SARS-CoV-2, Including the Delta and Omicron Variants. *Viruses* **14**, 1369 (2022).

101. Nguyen, P. L. Pathophysiological Roles of Histamine Receptors in Cancer Progression: Implications and Perspectives as Potential Molecular Targets. *Biomolecules* **11**, 1232 (2021).

102. Jiang, Y. *et al.* ALDH enzyme activity is regulated by Nodal and histamine in the A549 cell line. *Oncol Lett* **14**, 6955–6961 (2017).

103. Benarroch, E. E. CHAPTER 8 - NEUROTRANSMITTERS. in *Pharmacology and Therapeutics* (eds. Waldman, S. A. et al.) 91–113 (W.B. Saunders, 2009). doi:10.1016/B978-1-4160-3291-5.50012-3.

104. Kim, H.-J., Lee, P. C. W. & Hong, J. H. Lamin-A/C Is Modulated by the Involvement of Histamine-Mediated Calcium/Calmodulin-Dependent Kinase II in Lung Cancer Cells. *Int J Mol Sci* **23**, 9075 (2022).

105. Cai, W.-K. *et al.* Activation of histamine H4 receptors decreases epithelial-to-mesenchymal transition progress by inhibiting transforming growth factor-β1 signalling pathway in non-small cell lung cancer. *Eur J Cancer* **50**, 1195–1206 (2014).

106. Paltauf-Doburzynska, J., Frieden, M., Spitaler, M. & Graier, W. F. Histamine-induced Ca2+ oscillations in a human endothelial cell line depend on transmembrane ion flux, ryanodine receptors and endoplasmic reticulum Ca2+-ATPase. *J Physiol* **524**, 701–713 (2000).

107. Fitzsimons, C. P., Monczor, F., Fernández, N., Shayo, C. & Davio, C. Mepyramine, a histamine H1 receptor inverse agonist, binds preferentially to a G protein-coupled form of the receptor and sequesters G protein. *J Biol Chem* **279**, 34431–34439 (2004).

108. Lonchampt, M. O. *et al.* Histamine H1-receptors mediate phosphoinositide and calcium response in cultured smooth muscle cells-interaction with cicletanine (CIC). *Agents and Actions* **24**, 255–260 (1988).

109. Zappia, C. D. *et al.* Effects of histamine H1 receptor signaling on glucocorticoid receptor activity. Role of canonical and non-canonical pathways. *Sci Rep* **5**, 17476 (2015).

110. Huang, W.-C. *et al.* Histamine regulates cyclooxygenase 2 gene activation through Orai1-mediated NFκB activation in lung cancer cells. *Cell Calcium* **50**, 27–35 (2011).

111. Manohar, K. *et al.* FDA approved L-type channel blocker Nifedipine reduces cell death in hypoxic A549 cells through modulation of mitochondrial calcium and superoxide generation. *Free Radic Biol Med* **177**, 189–200 (2021).

112. Xu, P., Sriramula, S. & Lazartigues, E. ACE2/ANG-(1–7)/Mas pathway in the brain: the axis of good. *Am J Physiol Regul Integr Comp Physiol* **300**, R804–R817 (2011).

113. Simões e Silva, A. C. & Sampaio, W. O. The Role of Angiotensin–(1-7) in Cancer. *Angiotensin-(1-7)* 219–229 (2019) doi:10.1007/978-3-030-22696-1_14.

114. Kaschina, E. & Unger, T. Angiotensin AT1/AT2 receptors: regulation, signalling and function. *Blood Press* **12**, 70–88 (2003).

115. Kerneis, M., Ferrante, A., Guedeney, P., Vicaut, E. & Montalescot, G. Severe acute respiratory syndrome coronavirus 2 and renin-angiotensin system blockers: A review and pooled analysis. *Arch Cardiovasc Dis* **113**, 797–810 (2020).

116. Singhal, T. A Review of Coronavirus Disease-2019 (COVID-19). *Indian J Pediatr* **87**, 281–286 (2020).

117. Behl, T. *et al.* CD147-spike protein interaction in COVID-19: Get the ball rolling with a novel receptor and therapeutic target. *Sci Total Environ* **808**, 152072 (2022).

118. Lim, S., Zhang, M. & Chang, T. L. ACE2-Independent Alternative Receptors for SARS-CoV-2. *Viruses* **14**, 2535 (2022).

119. Gheblawi, M. *et al.* Angiotensin-Converting Enzyme 2: SARS-CoV-2 Receptor and Regulator of the Renin-Angiotensin System: Celebrating the 20th Anniversary of the Discovery of ACE2. *Circ Res* **126**, 1456–1474 (2020).

120. Ni, W. *et al.* Role of angiotensin-converting enzyme 2 (ACE2) in COVID-19. *Critical Care* **24**, 422 (2020).

121. South, A. M., Tomlinson, L., Edmonston, D., Hiremath, S. & Sparks, M. A. Controversies of renin–angiotensin system inhibition during the COVID-19 pandemic. *Nat Rev Nephrol* **16**, 305–307 (2020).

122. Magalhaes, G. S., Rodrigues-Machado, M. da G., Motta-Santos, D., Campagnole-Santos, M. J. & Santos, R. A. S. Activation of Ang-(1-7)/Mas Receptor Is a Possible Strategy to Treat Coronavirus (SARS-CoV-2) Infection. *Frontiers in Physiology* **11**, (2020).

123. Karnik, S. S., Singh, K. D., Tirupula, K. & Unal, H. Significance of angiotensin 1–7 coupling with MAS1 receptor and other GPCRs to the renin-angiotensin system: IUPHAR Review 22. *Br J Pharmacol* **174**, 737–753 (2017).

124. Gallagher, P. E. & Tallant, E. A. Inhibition of human lung cancer cell growth by angiotensin-(1-7). *Carcinogenesis* **25**, 2045–2052 (2004).

125. Burghi, V. *et al.* Validation of commercial Mas receptor antibodies for utilization in Western Blotting, immunofluorescence and immunohistochemistry studies. *PLOS ONE* **12**, e0183278 (2017).

126. Liu, C.-P. *et al.* Mechanism of [Ca2+]i rise induced by angiotensin 1-7 in MDCK renal tubular cells. *J Recept Signal Transduct Res* **32**, 335–341 (2012).

127. Burghi, V. *et al.* Participation of Gαi-Adenylate Cyclase and ERK1/2 in Mas Receptor Signaling Pathways. *Front Pharmacol* **10**, 146 (2019).

128. Rahimi, A., Sharifi, H. & Li, P. C. H. Cytosolic Calcium Measurement Utilizing a Single-Cell Biochip to Study the Effect of Curcumin and Resveratrol on a Single Glioma Cell. *Methods Mol Biol* **2689**, 13–25 (2023).

129. Chang, C.-W. *et al.* Cell culture model system utilizing engineered A549 cells to express high levels of ACE2 and TMPRSS2 for investigating SARS-CoV-2 infection and antiviral. Preprint at https://doi.org/10.1101/2021.12.31.474593 (2022).

130. Li, X., Xue, X. & Li, P. C. H. Real-time detection of the early event of cytotoxicity of herbal ingredients on single leukemia cells studied in a microfluidic biochip. *Integr. Biol.* **1**, 90–98 (2009).

131. Khamenehfar, A., Gandhi, M. K., Chen, Y., Hogge, D. E. & Li, P. C. H. Dielectrophoretic Microfluidic Chip Enables Single-Cell Measurements for Multidrug Resistance in Heterogeneous Acute Myeloid Leukemia Patient Samples. *Anal. Chem.* **88**, 5680–5688 (2016).

132. Starkus, J. *et al.* Diverse TRPV1 responses to cannabinoids. *Channels (Austin)* **13**, 172–191 (2019).

133. Lowin, T. & Straub, R. H. Cannabinoid-based drugs targeting CB1 and TRPV1, the sympathetic nervous system, and arthritis. *Arthritis Res Ther* **17**, 226 (2015).

Appendix A. Notes on experimental procedures

1. Do not leave the cryovial unattended during the cell thawing process. (It is important for cell viability that the cells are thawed and processed quickly – thawing only takes a few seconds). When 80% of the solution has thawed, it is ready for the next step.

2. You can confirm that the cells are completely detached from the plate by observing the cells under the microscope while swirling the plate.

3. FBS contains protease inhibitors, such as α-1 antitrypsin, that can deactivate trypsin. So the inhibitor must be deactivated by washing the cells with PBS before trypsinization.

4. To avoid cell clumping, do not agitate the cells by hitting or shaking the flask while waiting for the cells to detach. Cells that are difficult to detach may be placed at 37°C to facilitate dispersal.

5. Cells should be sub-cultured every 3-4 days when cell confluence reaches 80%.

6. A growing body of literature demonstrates that the passage number affects a cell line's characteristics over time. Cell lines at high passage numbers of experience alterations in morphology, response to stimuli, growth rate, and protein expression and transfection efficiency, as compared to lower-passage cells.

7. To prevent any damages to the PMT, ensure microphotometer dial is switched to “View” while the room light is on. When a red lamp is used, and during fluorescence measurement, the dial is switched to "Measure".

8. If an air bubble is observed during the loading of 70% ethanol, use suction to remove the air bubble. Then, allow the remaining ethanol to evaporate before repeating the step.

9. After successfully completion of the priming step by 70% ethanol, all subsequent steps should be swiftly performed to prevent the evaporation of residual ethanol that is left in channels, which would finally out defeat the purpose of ethanol priming.

10. While a cell pellet is re-suspended in the medium solution by pipetting it up and down, a P1000 micropipette must be used. The use of lower-volume micropipettes, such as the P200 or P10, can damage the cells and reduce their viability.

11. To test if the desired single cell appears to have adhered to the chamber of the microchip during the 10-min incubation period, an aliquot of medium solution can be removed or added to Reservoir 3 to confirm no change of cell position.

12. During the adjustment of the measurement window, ensure there is some space around the cell. It is because the cell may increase in size during the experiment.

13. Before adding test reagents to Reservoir 2, ensure that it is completely vacant by sucking out excess solution. This is to prevent dilution of the reagent concentration.

14. Don’t use strong acids (e.g., HCl) or strong bases (e.g., NaOH) to clean the reservoirs or chambers of the microfluidic chip. The soap used in this experiment has been made by adding 5mL of Sparkleen 1 (Fisherbrand) to 1L of warm water and then stored in a disposable syringe for easy injection inside the microfluidic reservoirs and channels.